THE ANALYSIS AND DESIGN OF A SHIP-CRADLE DECOUPLING SCHEME FOR DEEP SUBMERSIBE RECOVERY AT SEA.

Larry A. Dow

THE ANALYSIS AND DESIGN OF A SHIP-CRADLE DECOUPLING SCHEME FOR DEEP SUBMERSIBLE RECOVERY AT SEA

by

LARRY A. DOW

B.S., University of New Hampshire

(1968)

SUBMITTED IN PARTIAL FULFILLMENT OF

THE REQUIREMENTS FOR THE DEGREES OF

MASTER OF SCIENCE IN OCEAN ENGINEERING

AND

MASTER OF SCIENCE IN MECHANICAL ENGINEERING

at the

MASSACHUSETTS INSTITUTE OF TECHNOLOGY

May, 1973

THE ANALYSIS AND DESIGN OF A SHIP-CRADLE DECOUPLING SCHEME FOR DEEP SUBMERSIBLE RECOVERY AT SEA

by

LARRY A. DOW

Submitted to the Department of Ocean Engineering and to the Department of Mechanical Engineering in partial fulfillment of the requirements for the degree of Master of Science in Ocean Engineering and the degree of Master of Science in Mechanical Engineering.

ABSTRACT

An analysis is done of the motion of an underwater cradle for submerged recovery of the DSRV Alvin.

The cradle is modeled as a three degree of freedom system with four corner springs and includes heave pitch and roll motions. The surface ship Lulu is taken as the driving force that couples energy into the cradle through the springs. Hydrodynamic damping values are found by a 64 section finite element analysis and are compared to corresponding linear approximations.

Solution of the resulting equations was accomplished using a Runge-Kutta numerical integration method developed at M.I.T.

The solution showed that four soft corner springs in the range of 20-50 lbf will substantially decrease the transmitted ship motion. Additionally, the results indicate that the pitch and roll natural frequency is higher than the heave natural frequency and consequently is the limiting design consideration.

The results of the analysis are discussed and several possible approaches are considered for producing a soft spring constant while at the same time supporting the high static load of the cradle weight.

Thesis Supervisor: J. H. Evans
Title: Professor of Ocean Engineering

ACKNOWLEDGEMENTS

The author wishes to express thanks to the following people who provided technical advice and encouragement and thus contributed to the thesis:

Professor J. H. Evans and Professor R. S. Sidell, who, as Thesis Supervisor and Department Reader, respectively, offered insight and valuable criticism. As a result many pitfalls were avoided during the development of this analysis.

My new wife, Carla, who tolerated my moods, typed the first draft, and provided encouragement during numerous setbacks in my work. To her goes special thanks.

Mrs. Jack ("Sam") Price, who offered professional advice on its format and organization and who efficiently typed the final draft.

TABLE OF CONTENTS

LIST OF FIGURES

NOMENCLATURE

Symbol	Interpretation
x	Forward direction of Lulu
y	Downward motion of Lulu
z	Athwartships of Lulu
Y_0	Maximum heave amplitude of Lulu
θ_0	Maximum pitch angle of Lulu
Φ_0	Maximum roll angle
θ	Cradle pitch angle
ϕ	Cradle roll angle
ω_1	Heave and pitch frequency of Lulu
ω_2	Roll frequency of Lulu
ρ	Density of seawater
C_D	Coefficient of viscous damping
M_0	Mass of cradle
M_a	Added mass of cradle
M_T	Total mass of cradle
I_{01}	Actual pitch inertia of cradle
I_{a1}	Added pitch inertia of cradle
I_1	Total pitch inertia
I_{02}	Actual roll inertia of cradle
I_{a2}	Added roll inertia of cradle
I_2	Total roll inertia of cradle
L	Length of cradle
W	Width of cradle

Symbol	Interpretation
Percent	Percent deviation in springs
K_1 - K_4	Four cradle support springs
α	Fore and aft sway
B	Transverse sway
α_1	Coefficient of real part of complex pole
β_1	Coefficient of imaginary part of complex pole
β_m	Bulk modulus
Q_m	Flow to load
P_m	Load pressure
R	Proportional control constant
S	Integral control constant
A	Area of piston
V	Volume of piston
K_e	Cylinder compliance
K_{et}	Total compliance
K_{Ox}	Flow sensitivity of valve gain
K_{Op}	Negative slope of P_m versus Q_m curve
F_i	Valve forces
t	time
C(t)	Set point input to P I control
D	Damping factor
a_{11}-a_{44}	The sixteen elements making up quadrant one of the cradle's projected area
δ	Spring stretch

CHAPTER I.

INTRODUCTION

The handling of heavy objects through the air-sea interface is not a new or unique problem and has been studied many times in the past. The deep submergence research vehicle (DSRV) Alvin owned by the U.S. Navy and operated by Woods Hole Oceanographic Institute (WHOI) is most likely the DSRV with the world's best record for successful dives completed. The submersible is handled by its support ship, a catamaran named Lulu and is transported to and from the open ocean dive site between Lulu's twin hulls.

The launching and retrieving operation is accomplished with a great deal of care, Alvin being initially positioned on her 30-ton capacity cradle just aft of amidships. The cradle, (Figure 1), is supported at its four corners by chain hoists which are two-blocked such that the cradle is at deck level during transit. This allows easy maintenance, repairs and manning of Alvin.

During launching, the catamaran lies with its stern to the seas, the cradle is then lowered and the floating submersible clears Lulu with the aid of Alvin's screw and numerous snubber lines. Recovery is the reverse of the operation, Alvin surfacing well away from Lulu, closing Lulu, and finally driving between Lulu's hulls and being manually positioned over the submerged cradle. Last, when the wave timing is correct, the cradle-submersible combination is raised clear of the water.

This method of launching and retrieval has allowed reasonably routine operations to occur in sea states up to three, with occasional sea state four retrieval due to emergency conditions.

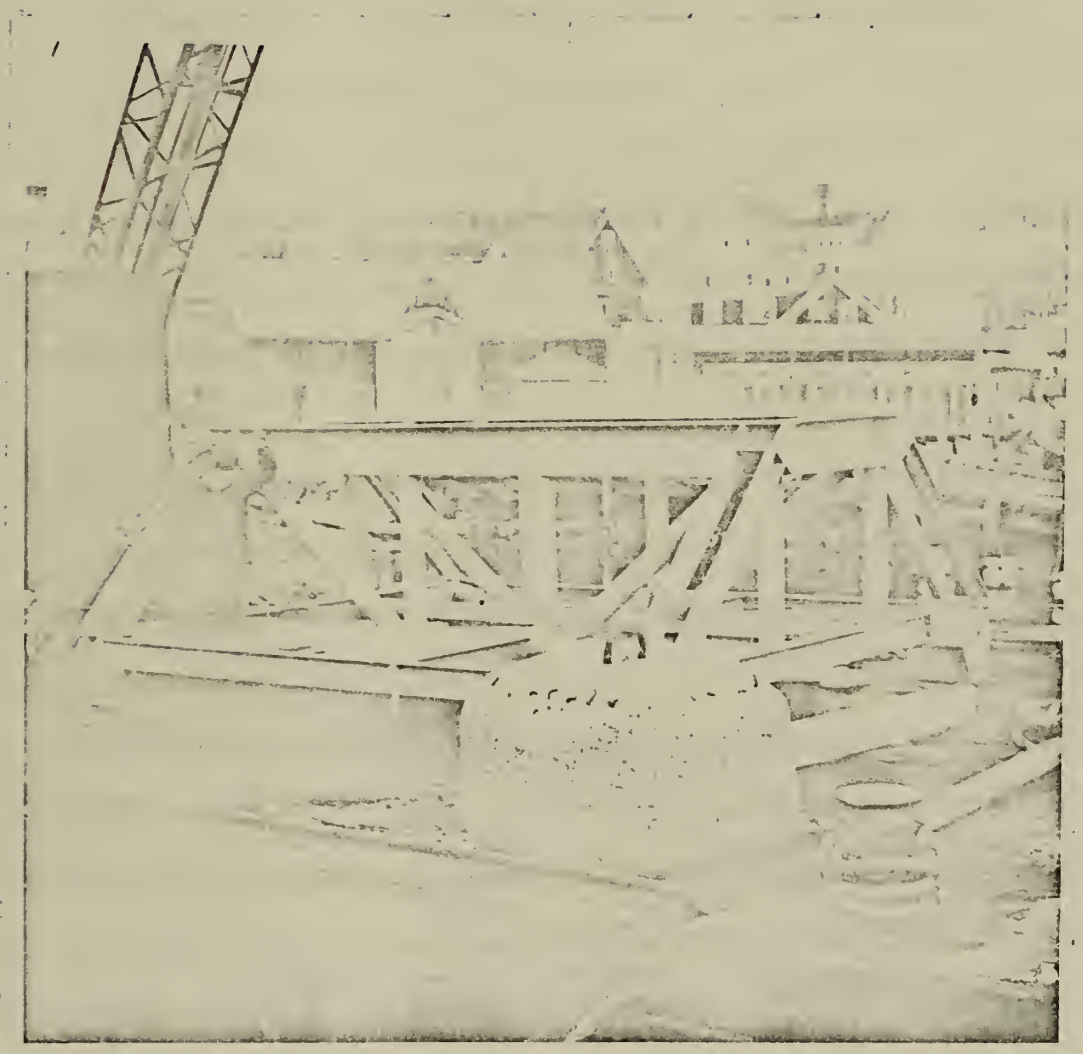

Figure 1.

Without going into a discussion of sea state probabilities, it is well known that along the north Atlantic off Cape Cod the sea state will frequently go from state three to state four due to a prevailing southwest wind which increases from ten knots in the morning to about 20 in the afternoon. Sea state four makes for a very difficult recovery should it occur during the time of a dive. The problem here really is that once the Alvin is in position to be hoisted aboard, the relative motion between Alvin, the cradle, and Lulu could cause very high and damaging shock loading on Alvin, the hoist, or the cradle. This loading could possibly result in severe damage to Alvin, or even another loss.

Clearly then, a smooth docking to a stationary cradle followed by a rapid hoisting through the air-sea interface would be highly desirable and would virtually eliminate shock loading and consequent damage.

Fortunately, the Alvin's cradle consists of four 120' lengths of chain and four synchronized wildcats. If the cradle were lowered to approximately 100' below the surface, the surface wave effect would be virtually inefective on Alvin and it would be possible to dock or depart from the cradle without the fear of poor surface conditions. The problem which appears to be the limiting factor is the motion of the cradle itself. This motion is nearly the same as that of Lulu due to the inelastic chains which connect the two. Some work has been done to show the transmitted surface motion that the cradle would feel. It has been generally concluded that if members more elastic than chains were used, perhaps the cradle motion could be uncoupled from the Lulu and the Alvin could dock with a virtually motionless cradle at 100' and then be hauled to the surface rapidly and safely through the air-sea interface.

The complete analysis of the Lulu-cradle interaction is the primary concern in this thesis.

CHAPTER II.

THEORY AND DEVELOPMENT OF EQUATIONS OF MOTION

To this time the ship cradle interaction motion has been studied using a simple model shown in Figure 2. While this model applies very well to a system with a single support it does not predict the motion of a four point suspended cradle with ship pitch, roll, and heave.

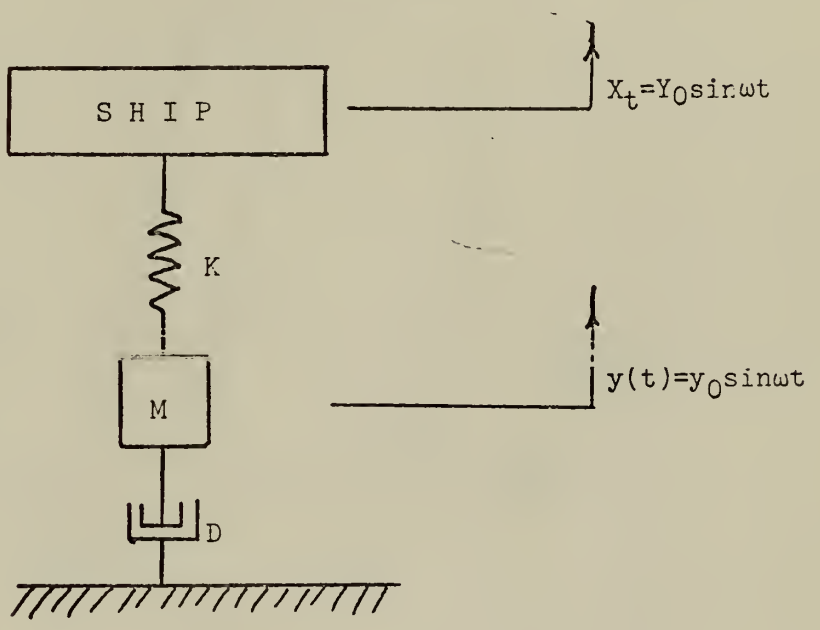

Figure 2.

Looking at Figure 3 it is apparent that the motions of a cradle beneath a ship are extremely complex. The cradle can exhibit vertical motion (y), pitch (θ), roll (ϕ), fore and aft sway (α), transverse sway (β), twisting about the y axis, as well as horizontal motion in the x direction. In effect, all six degrees of freedom can be achieved with the cradle. Fortunately, to somewhat simplify the problem, fore and aft sway (α),

Figure 3.

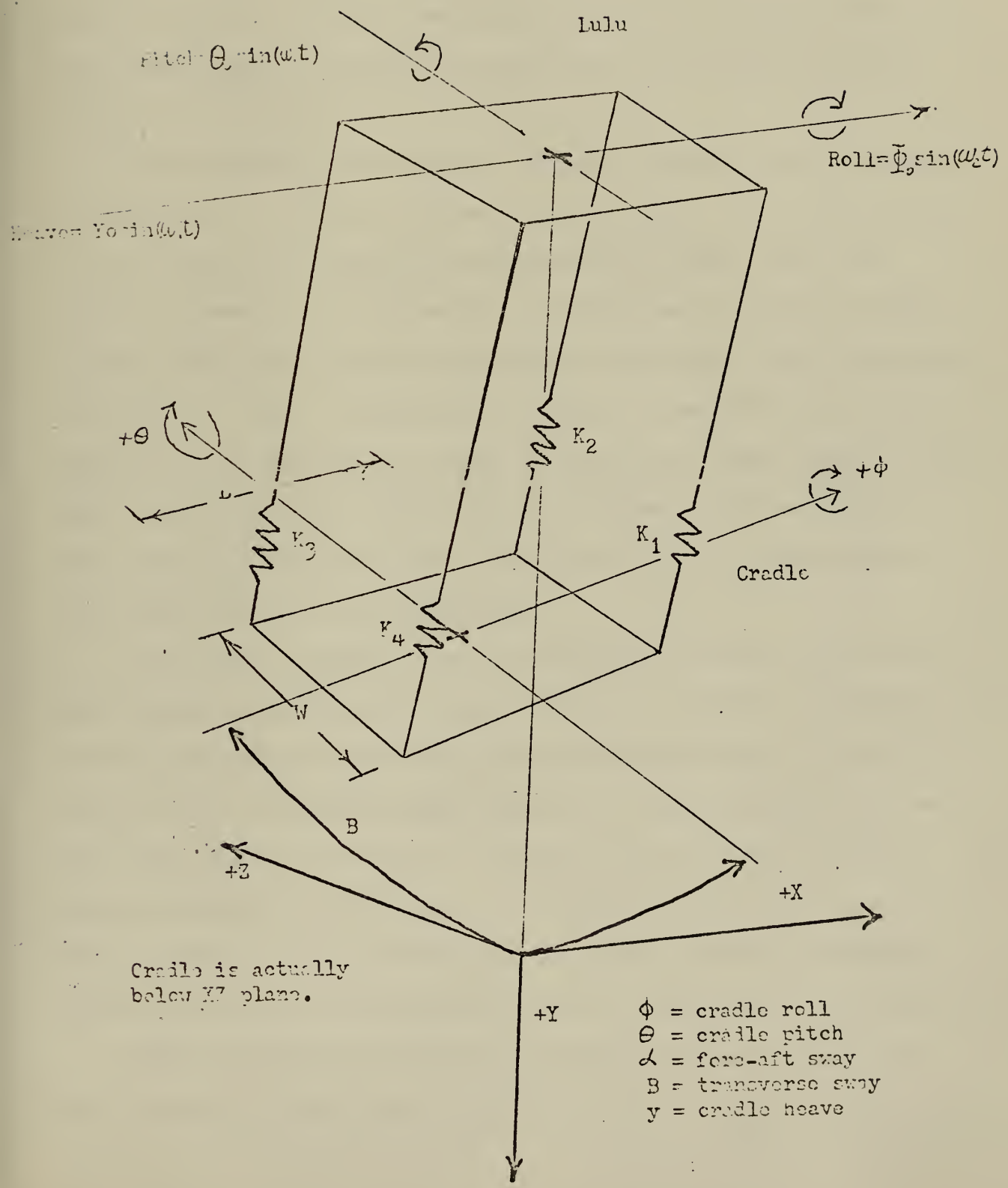
Lulu
Pitch=θ₀sin(ω₁t)
Roll=Φ₀sin(ω₂t)
Heave=Y₀sin(ω₃t)
+θ
+ϕ
K₂
K₃
K₁
K₄
Cradle
W
B
+Z
+X
+Y
Cradle is actually below XZ plane.
ϕ = cradle roll
θ = cradle pitch
α = fore-aft sway
B = transverse sway
y = cradle heave

transverse sway (β), and twist were experimentally found to be insignificant.

Consequently, the problem to be solved is a three degree of freedom one with roll (ϕ), pitch (θ), and heave (y), and where all three modes of motion can transfer energy back and forth thus contributing to the complexity of the problem.

Before beginning the modeling the initial conditions must be defined. To begin with, the cradle is assumed to be of length l = 17.5 feet, width w = 16.3 feet, with a weight of approximately 508 slugs. Since the reference material has indicated that a possible mode of operation would be with a flat plate affixed to the bottom of the cradle, this is the mode chosen for our model. Consequently the cradle is assumed to be a rectangular flat plate with mass equivalent to that of the cradle alone. In the final analysis it will be shown that the added mass terms associated with the cradle so overpower the actual mass that the exact configuration of the cradle structure is inconsequential.

It was first necessary to pick an adequate co-ordinate system which would accurately describe the system and make it possible to completely position the cradle knowing only three co-ordinates--heave (y), pitch (θ), and roll (ϕ). A reference system (Figure 4), fixed above the cradle was chosen with X positive forward, Y positive down and Z positive to port. Using the conventional right hand rule, positive θ and positive ϕ are as shown in Figure 4. As is conventional in dynamic analysis the cradle is given an instantaneous displacement positive y, positive θ, and positive ϕ.

Since the equations of the system which are being dealt with are quite complex with many terms, it will be convenient to set up the

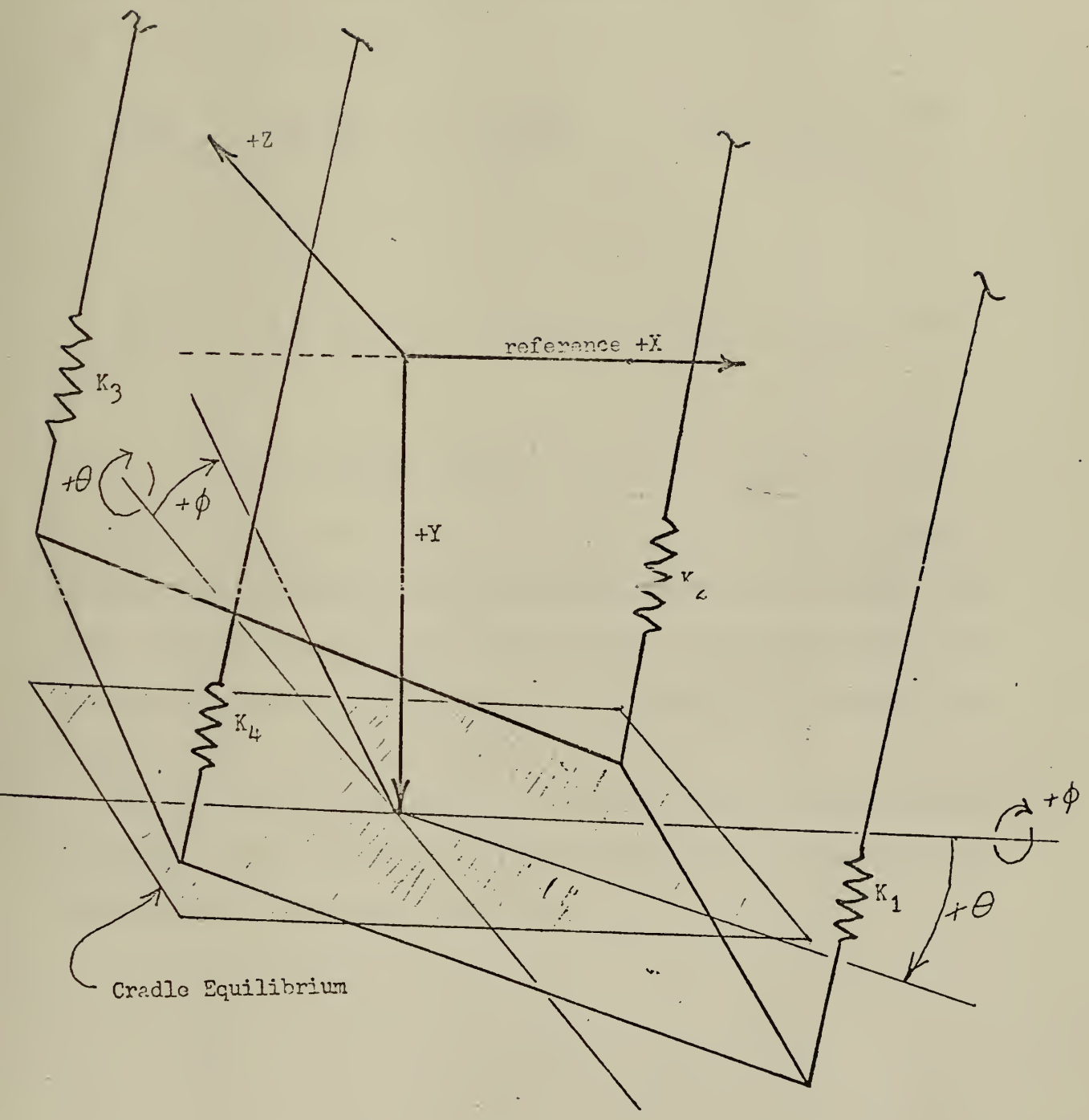

Figure 4.

resultant equation in standard state variable form consisting of six first order differential equations and an output expression. The most general form of such an equation is

$$\begin{bmatrix} \dot{X}_1(t) \\ \dot{X}_2(t) \\ \cdot \\ \cdot \\ \cdot \\ \cdot \\ \cdot \\ \dot{X}_n(t) \end{bmatrix} = \begin{bmatrix} A_{11}\ A_{12}\cdots\cdots A_{1n} \\ A_{21}\ A_{22}\cdots\cdots \\ \cdot \\ \cdot \\ \cdot \\ \cdot \\ \cdot \\ A_{n1}\ A_{n2}\cdots\cdots A_{nn} \end{bmatrix} \begin{bmatrix} X_1(t) \\ X_2(t) \\ \cdot \\ \cdot \\ \cdot \\ \cdot \\ \cdot \\ X_n(t) \end{bmatrix} + \begin{bmatrix} b_{11}b_{12}\cdots\cdots b_{1n} \\ \cdot \\ \cdot \\ \cdot \\ \cdot \\ \cdot \\ \cdot \\ b_{n1}\cdots\cdots\cdots b_{nr} \end{bmatrix} \begin{bmatrix} U_1(t) \\ \cdot \\ \cdot \\ \cdot \\ \cdot \\ \cdot \\ \cdot \\ U_r(t) \end{bmatrix}$$

or

$$\overline{\dot{X}}(t) = \overline{A}\overline{X}(t) + \overline{B}\overline{u}(t)$$

where $\overline{A}$ is the $\overline{N} \times \overline{N}$ system matrix with $\overline{B}$ an $\overline{N} \times \overline{r}$ control matrix. Strictly speaking, this above representation applies only to a N^{th} order linear equations, however, since there will be a multitude of terms, both linear and nonlinear, it will be a good bookkeeping aid to arrange terms as such.

The basic equation of motion for a spring, mass, and damper system is used here. Development of the equations of motion is begun with the consideration of this free body diagram.

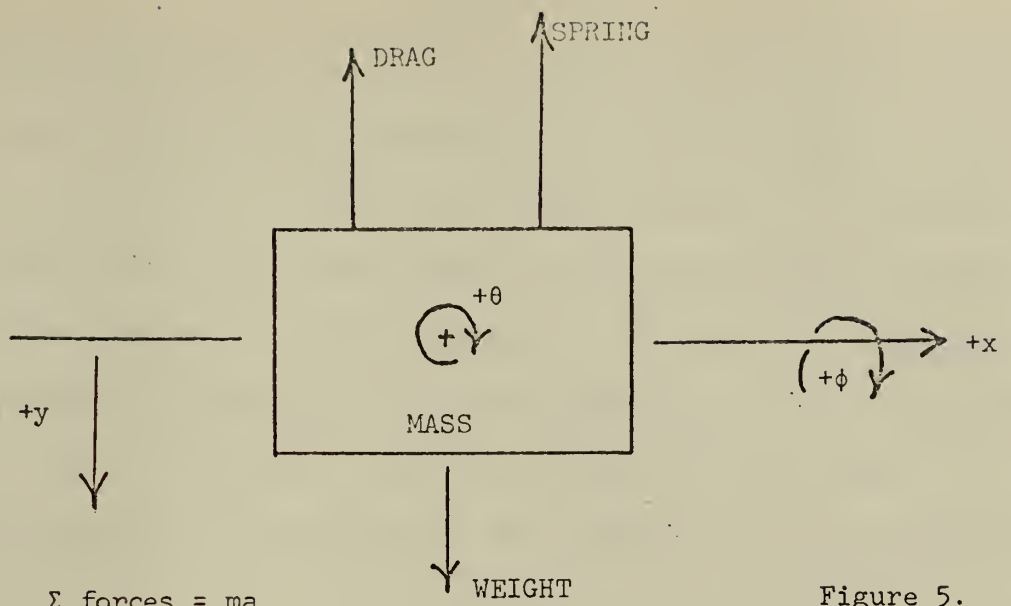

where: Σ forces = ma Figure 5.

or:

$$m\ddot{y} = - F_{drag} - F_{spring} + force\ (exciting)$$

and is the case of three degrees of freedom

$$m\ddot{y} = - F_{drag} - F_{spring} + F_{exciting}\ (\bar{y})$$

$$I_1\ddot{\theta} = - F_{drag} - F_{spring} + F_{exciting}\ (\theta_0)$$

$$I_2\ddot{\phi} = - F_{drag} - F_{spring} + F_{exciting}\ (\Phi_0).$$

Each term will be discussed independently.

The Spring Force

The four springs (chains) at the corners of the cradle are the major factor in decoupling the surface motion from the cradle. The spring force is proportional to its stretch and this stretch may well be different for each of the four springs. This is one of the mechanisms by which energy is transferred from one mode, such as heave, to pitch or roll. Ideally, if all four springs were equal and the cradle were given a pure pitch, roll, or heave motion, then the other modes would not be excited and you would

have simply three uncoupled systems. However, considering the inexactness of the Real World, the cross coupled damping, and the exterior forces, it would be unrealistic to perform such a simple analysis. In actuality the ship pitches, rolls, and heaves about an equilibrium position as does the cradle. The stretch of the four springs is defined as the difference in position between the position of the ship and the position of the cradle relative to their respective equilibrium for each motion mode.

The respective stretches of the four springs K_1, K_2, K_3, and K_4 are as follows:

$$\delta_1 = (y - Y_0 \sin\omega_1 t) + (L/2\theta - L/2\theta_0 \sin\omega_1 t) + (W/2\phi - w/2\Phi_0 \sin\omega_2 t)$$

$$\delta_2 = (y - Y_0 \sin\omega_1 t) + (L/2\theta - L/2\theta_0 \sin\omega_1 t) - (W/2\phi - w/2\Phi_0 \sin\omega_2 t)$$

$$\delta_3 = (y - Y_0 \sin\omega_1 t) - (L/2\theta - L/2\theta_0 \sin\omega_1 t) - (W/2\phi - w/2\Phi_0 \sin\omega_2 t)$$

$$\delta_4 = (y - Y_0 \sin\omega_1 t) - (L/2\theta - L/2\theta_0 \sin\omega_1 t) + (W/2\phi - w/2\Phi \sin\omega_2 t)$$

This is assuming that Y_0, θ_0, and Φ_0, are the ship's pitch, roll, and heave.

Carrying this a bit further, when the stretches are multiplied by their spring constants, we get the respective restoring spring forces and moments in general form.

The equation for heave--

$$m\ddot{y} = - K_1\delta_1 - K_2\delta_2 - K_3\delta_3 - K_4\delta_4$$

The equation for pitch--

$$I_1\ddot{\theta} = - K_1\frac{L}{2}\delta_1 - K_2\frac{L}{2}\delta_2 + K_3\frac{L}{2}\delta_3 + K_4\frac{L}{2}\delta_4$$

The equation for roll--

$$I_2\ddot{\phi} = + K_2 \frac{W}{2} \delta_2 + K_3 \frac{W}{2} \delta_3 - K_1 \frac{W}{2} \delta_1 - K_4 \frac{W}{2} \delta_4$$

or plugging in δ's,

heave equation--

$$m\ddot{y} + K_1\delta_1 + K_2\delta_2 + K_3\delta_3 + K_4\delta_4 = 0$$

Plugging in:

$$m\ddot{y}_2 = - K_1[(y_1 - Y_0\sin\omega_1 t) + (\frac{L}{2} y_3 - \frac{L}{2} \theta_0\sin\omega_1 t) + (\frac{W}{2} y_5 - \frac{W}{2} \Phi_0 \sin\omega_2 t)]$$

$$- K_2[(y_1 - Y_0\sin\omega_1 t) + (\frac{L}{2} y_3 - \frac{L}{2} \theta_0\sin\omega_1 t) - (\frac{W}{2} y_5 - \frac{W}{2} \Phi_0\sin\omega_2 t)]$$

$$- K_3[(y_1 - Y_0\sin\omega_1 t) - (\frac{L}{2} y_3 - \frac{L}{2} \theta_0\sin\omega_1 t) - (\frac{W}{2} y_5 - \frac{W}{2} \Phi_0\sin\omega_2 t)]$$

$$- K_4[(y_1 - Y_0\sin\omega_1 t) - (\frac{L}{2} y_3 - \frac{L}{2} \theta_0\sin\omega_1 t) + (\frac{W}{2} y_5 - \frac{W}{2} \Phi_0\sin\omega_2 t)]$$

pitch equation--

$$I_1\ddot{y}_4 = + K_3 \frac{L}{2}[(y_1 - Y_0\sin\omega_1 t) - (\frac{L}{2} y_3 - \frac{L}{2} \theta_0\sin\omega_1 t) - (\frac{W}{2} y_5 - \frac{W}{2} \Phi_0\sin\omega_2 t)]$$

$$+K_4 \frac{L}{2}[(y_1 - Y_0\sin\omega_1 t) - (\frac{L}{2} y_5 - \frac{L}{2} \theta_0\sin\omega_1 t) + (\frac{W}{2} y_5 - \frac{W}{2} \Phi_0\sin\omega_2 t)]$$

$$-K_1 \frac{L}{2}[(y_1 - Y_0\sin\omega_1 t) + (\frac{L}{2} y_3 - \frac{L}{2} \theta_0\sin\omega_1 t) + (\frac{W}{2} y_5 - \frac{W}{2} \Phi_0\sin\omega_2 t)]$$

$$-K_2 \frac{L}{2}[(y_1 - Y_0\sin\omega_1 t) + (\frac{L}{2} y_3 - \frac{L}{2} \theta_0\sin\omega_1 t) - (\frac{W}{2} y_5 - \frac{W}{2} \Phi_0\sin\omega_2 t)]$$

roll equation--

$$I_2\ddot{y}_6 = - K_1\frac{W}{2}[(y_1 - Y_0\sin\omega_1 t) + (\frac{L}{2} y_3 - \frac{L}{2} \theta_0\sin\omega_1 t) + (\frac{W}{2} y_5 - \frac{W}{2} \Phi_0\sin\omega_2 t)]$$

$$-K_4\frac{W}{2}[(y_1-Y_0\sin\omega_1 t) - (\frac{L}{2}y_3 - \frac{L}{2}\theta_0\sin\omega_1 t) + (\frac{W}{2}y_5 - \frac{W}{2}\Phi_0\sin\omega_2 t)]$$

$$+K_2\frac{W}{2}[(y_1-Y_0\sin\omega_1 t) + (\frac{L}{2}y_3 - \frac{L}{2}\theta_0\sin\omega_1 t) - (\frac{W}{2}y_5 - \frac{W}{2}\Phi_0\sin\omega_2 t)]$$

$$+K_3\frac{W}{2}[(y_1-Y_0\sin\omega_1 t) - (\frac{L}{2}y_3 - \frac{L}{2}\theta_0\sin\omega_1 t) - (\frac{W}{2}y_5 - \frac{W}{2}\Phi_0\sin\omega_2 t)]$$

Driving Force

The force which excites the cradle is transferred through the springs to the cradle. In this analysis it is assumed that Lulu is heaving and pitching sinusoidal with the same frequency ω_1, and amplitudes Y_0 and θ_0, respectively. Additionally, it is assumed that Lulu is rolling sinusoidally with amplitude Φ_0 and frequency ω_2.

Drag Forces

This is the most difficult set of terms to analyze since due to the low Reynold's numbers involved the drag forces are primarily caused by hydrodynamic form drag rather than viscous drag and are nonlinear. In addition, for geometric shapes with hard edges the drag coefficients are generally independent of Reynold's numbers.

The general equation describing drag forces on such a shape is given as Drag = $\frac{1}{2}\rho A_c Cd V$, and it is in this where we find the problem. If drag is to always oppose motion as it does here, the equation above should actually be written Drag = $\frac{1}{2}\rho A_c Cd|V|V$, which will preserve the correct sign.

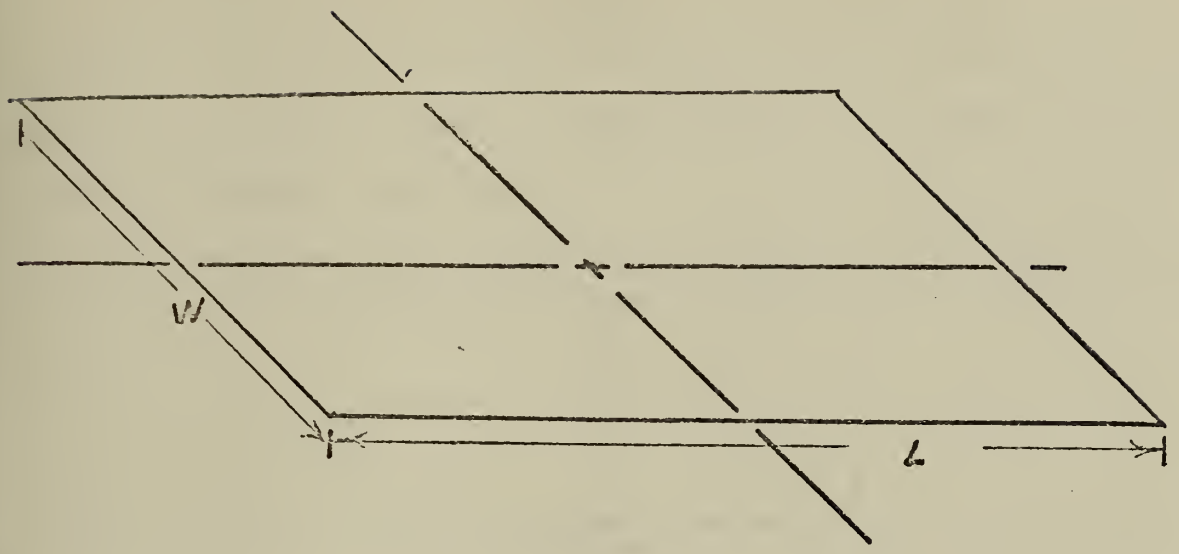

Figure 6.

Initially an exact attempt at the solution was tried. Inasmuch as a differential element of drag is defined in quadrant (1) of Figure 6 as

$$d(\text{drag}) = \tfrac{1}{2}\rho C_D dxdz(\dot{y}+x\dot{\theta}\cos\phi\cos\theta+z\dot{\phi}\cos\phi\cos\theta)\left|\dot{y}+x\dot{\theta}\cos\phi\cos\theta+z\dot{\phi}\cos\phi\cos\theta\right|.$$

then the total drag on quadrant (1) would logically be

$$\text{DRAG} = \int_0^{L/2}\int_0^{W/2} \tfrac{1}{2}\rho C_D dxdz(\dot{y}+x\dot{\theta}\cos\theta\cos\phi+z\dot{\phi}\cos\theta\cos\phi)\left|\dot{y}+x\dot{\theta}\cos\theta\cos\phi+z\dot{\phi}\cos\theta\cos\phi\right|.$$

This approach could be pursued to an exact solution if an identity for $(A+B+C)|A+B+C|$ was obtainable. However, $(A+B+C)\,|A+B+C|$ only equals $(A+B+C)\,(A+B+C)$ when $(A+B+C)$ is a positive number. The determination of the exact sign of $(A+B+C)$ or $(\dot{y}+x\dot{\theta}\cos\theta\cos\phi+z\dot{\phi}\cos\theta\cos\phi)$ can only be obtained when a known value of X, or Z is available. Consequently, if X and Z are in the integrand they cannot be assigned a specific value as they vary from

0 to L/2 and W/2 respectively. Thus, as mathematically satisfying as an exact equation for drag would be, it is alas, impossible to obtain. Due to this, a more straight forward yet more tedious finite element method was used to approximate drag forces.

The cradle was first divided up into four quadrants as shown below:

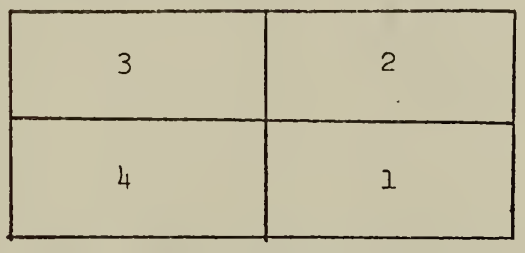

Figure 7.

Using the sign convention previously described, the velocities of any point in the four quadrants are as follows:

$$V_1 = (\dot{y} + x\,\dot{\theta}\cos\theta\cos\phi + z\dot{\phi}\cos\theta\cos\phi)$$

$$V_2 = (\dot{y} + x\,\dot{\theta}\cos\theta\cos\phi - z\dot{\phi}\cos\theta\cos\phi)$$

$$V_3 = (\dot{y} - x\,\dot{\theta}\cos\theta\cos\phi - z\dot{\phi}\cos\theta\cos\phi)$$

$$V_4 = (\dot{y} - x\,\dot{\theta}\cos\theta\cos\phi + z\dot{\phi}\cos\theta\cos\phi).$$

Each quadrant is then divided into sixteen areas and the drag is calculated for each one as shown for element a_{22} below.

Drag element a_{22}

$$= \tfrac{1}{2} \rho C_D \text{ Area } (a_{22}) \, Va_{22} |Va_{22}|$$

$$\text{Area } a_{22} = \frac{W}{8} \cdot \frac{L}{8}$$

$$V_{22} = (\dot{y} + \frac{3}{16} L\dot{\theta}\cos\theta\cos\phi + \frac{3}{16} W\dot{\phi}\cos\theta\cos\phi)$$

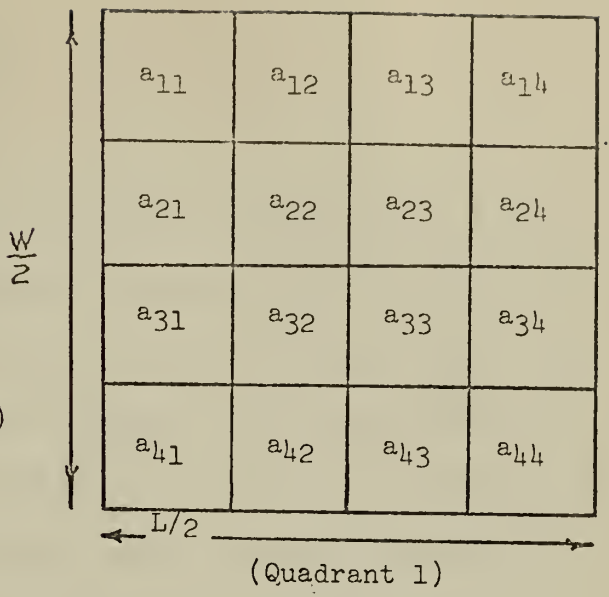

Figure 8.

$$\text{Drag}(a_{22}) = \tfrac{1}{2} \rho C_D (\frac{W}{8} \cdot \frac{L}{8})(\dot{y} + \frac{3}{16} L\dot{\theta}\cos\theta\cos\phi + \frac{3}{16} W\dot{\phi}\cos\theta\cos\phi) |\dot{y} + \frac{3}{16} L\dot{\theta}\cos\theta\cos\phi + \frac{3}{16} W\dot{\phi}\cos\theta\cos\phi|$$

Hence, the velocity is assumed to be fixed over the entire element and thus, so is the sign of the drag. Ideally, as the number of elements goes up, the possibility of the total velocity changing sign in an element goes down until, in the limit, you have numerically integrated the whole surface to an exact result. In this analysis 64 elements are taken each time step and added together to produce the resultant drag.

Pitch and roll drag are calculated in much the same way but with the added complication that each drag element acts through a finite moment arm to produce the drag in terms of foot lbs. One difference is the proper description of the velocity of the element which for our same element a_{22} would be

$$Va_{22} = (\dot{y}\cos\theta\cos\phi + \frac{3}{16} L\dot{\theta} + \frac{3}{16} W\dot{\phi}).$$

The computer subroutines for calculating the drag forces are given in the Appendix.

Inertia Forces

In cases where the relative velocity between a submerged body and its surrounding water does not remain constant, additional forces come into play as a result of the acceleration of the mass of water entrained by the body. This added mass depends on the physical dimensions of the body as well as its mode of motion. The actual body mass plus the added mass is called the virtual, induced, or total mass. Similarly, there are added moments of inertia terms which accompany the body's angular acceleration. Consequently, for a long flat plate of dimensions such as

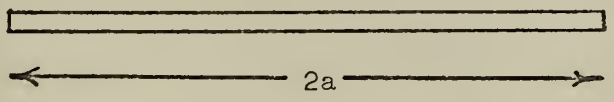

the added mass of the entrained water for motion perpendicular to the plane of the cradle is defined as $M_a = \rho\pi a^2$, or in our case $a = \frac{W}{2}$ depth = L so $M_a = \frac{1}{4}\rho\pi W^2 L$. The total mass is then actual mass plus added mass

$$M_T = M(\text{actual}) + M\ (\text{added})$$

$$M_T = 508 + \tfrac{1}{4}\rho\pi W^2 L.$$

The added roll moment of inertia due to the entrained water is defined as

or in our case $I_{a_2} = 1/8\rho\pi a^4$,

$$I_{a_2} = 1/8\rho\pi(\frac{W}{2})^4 L.$$

The total roll moment of inertia is then

$$I_2 = \frac{MW^2}{12} + \frac{1}{8}\rho\pi\frac{W^4}{16}L.$$

Similarly, for pitch it is

$$I_1 = \frac{ML^2}{12} + \frac{1}{8}\rho\pi\frac{L^4}{16}W.$$

Static Forces

These forces consisting of buoyancy and weight are constant and thus do not enter into the equation in any way.

Overview

The equations developed to this point are nonlinear due to the drag terms but fortunately can be solved by various numerical methods of integration. The equations, arranged in state variable form are shown in Figure 9. It is important to note that the drag terms shown are extremely complex and are functions of five of the six state variables. More specifically, the heave, pitch, and roll drag forces are functions of the following: y(2), vertical velocity of cradle; y(3), the cradle pitch angle; y(4), the cradle pitch angular velocity; y(5), the cradle roll angle; and y(6), the cradle roll angular velocity. Additionally, the heave, pitch and roll drags are different functions of these variables.

The forms of these functions have been explained in previous paragraphs.

$$
\begin{bmatrix} \dot{Y}_1 \\ \dot{Y}_2 \\ \dot{Y}_3 \\ \dot{Y}_4 \\ \dot{Y}_5 \\ \dot{Y}_6 \end{bmatrix} =
\begin{bmatrix}
0 & 1 & 0 & 0 & 0 & 0 \\
-\frac{(K_1+K_2+K_3+K_4)}{M_T} & \text{-DRAG (heave)} \\ & f(y(2),y(3),y(4),y(5),y(6)) \\ & \text{finite element} & -\frac{(K_1L+K_2L-K_3L-K_4L}{2M_T} & 0 & -\frac{(-K_1W-K_2W-K_3W+K_4W)}{2M_T} & 0 \\
0 & 0 & 0 & 1 & 0 & 0 \\
-\frac{(K_3L-K_4L+K_1L+K_2L)}{2I_1} & \text{-DRAG (pitch)} \\ & f(y(2),y(3),y(4),y(5),y(6)) \\ & \text{finite element} & -\frac{(K_3L^2+K_4L^2+K_1L^2+K_2L^2)}{4I_1} & 0 & -\frac{(+K_3LW-K_4LW+K_1LW-K_2WL)}{4I_1} & 0 \\
0 & 0 & 0 & 0 & 0 & 1 \\
-\frac{(K_1W+K_4W-K_2W-K_3W}{2I_2} & \text{-DRAG (roll)} \\ & f(y(2),y(3),y(4),y(5),y(6)) \\ & \text{finite element} & -\frac{(K_1WL-K_4WL-K_2WL+K_3WL)}{4I_2} & 0 & -\frac{(K_1W^2+K_4W^2+K_2W^2+K_3W^2)}{4I_2} & 0
\end{bmatrix}
\begin{bmatrix} Y_1(y) \\ Y_2(\dot{y}) \\ Y_3(\theta) \\ Y_4(\dot{\theta}) \\ Y_5(\phi) \\ Y_6(\dot{\phi}) \end{bmatrix}
+
\begin{bmatrix}
0 & 0 & 0 \\
\frac{(K_1+K_2+K_3+K_4)}{M_T} & \frac{(K_1L+K_2L-K_3L-K_4L)}{2M_T} & \frac{(K_1W-K_2W-K_3W+K_4W)}{2M_T} \\
0 & 0 & 0 \\
\frac{(-K_3L-K_4L+K_1L+K_2L)}{2I_1} & \frac{(K_3L^2+K_4L^2+K_1L^2+K_2L^2)}{4I_1} & \frac{(K_3LW-K_4LW+K_1WL-K_2WL)}{4I_1} \\
0 & 0 & 0 \\
\frac{(K_1W+K_4W-K_2W-K_3W)}{2I_2} & \frac{(K_1WL-K_4WL-K_2WL+K_3W)}{4I_2} & \frac{(K_1W^2+K_4W^2+K_2W^2+K_3W^2)}{4I_2}
\end{bmatrix}
\begin{bmatrix} Y_0 \sin\omega_1 t \\ \theta_0 \sin\omega_1 t \\ \phi_0 \sin\omega_2 t \end{bmatrix}
$$

Figure 9.

CHAPTER III.

DEVELOPMENT OF LINEAR APPROXIMATIONS

As discussed previously, the equations as developed are nonlinear. Unfortunately, this fact results in the necessity of a brute force approach to the solution. That is, the well developed test and analysis methods which apply to systems of linear equations cannot be used to draw general conclusions about a nonlinear system. Consequently, linear approximations for the drag terms would be helpful only if they were shown to give reasonable results when compared to the exact approach.

Ideally, the nonlinear drag terms, which now are functions of five of the six state variables, should be reduced to functions of only one velocity term. Actually, it would be reasonable to expect the majority of a particular drag term to be caused by the velocity mainly associated with that term. That is, heave drag should mainly be caused by heave velocity, pitch drag by pitch angular velocity, and similarly, roll drag by roll angular velocity.

Therefore, using this as an initial approach, the single variable heave drag equation might be:

$$\text{Drag (heave)} = \tfrac{1}{2}\ \rho C_D W L \dot{y}^2$$

The equation for pitch drag would be somewhat more complicated and would be calculated as shown in Figure 10.

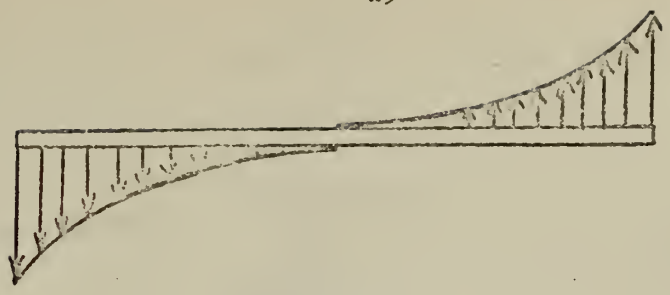

Figure 10.

$$d\ (\text{drag}) = 2 \times \tfrac{1}{2}\, \rho C_D W dX (X\dot{\theta})(X\dot{\theta})X$$

$$\text{DRAG} = \int_0^{L/2} \tfrac{1}{2}\rho C_D W x^3 \dot{\theta}^2 dx$$

$$\text{DRAG (pitch)} = \frac{\rho C_D W L^4 \dot{\theta}^2}{64}$$

Similarly the equation for roll drag is

$$\text{DRAG (roll)} = \frac{\rho C_D W L^4 \dot{\phi}^2}{64}$$

As yet, even these equations are nonlinear due to their squared velocity terms.

Several approximations to velocity squared damping have been used in the past. One of the commonly used electrical approximations consists of equating the energy dissipated by a current squared resistor to the energy dissipated by a linear resistor when both are driven by a sinusoidal current source. When this is done the I^2 term is in effect related to a constant multiplied by a single power of I. The constant which results is $\frac{8}{3\pi} I_0 \omega_1$ where I_0 is the maximum current value and ω_1 is the driving frequency.

Therefore, if we consider the sea as a velocity squared damper, a reasonable approximation to heave drag would be

$$\tfrac{1}{2}\rho C_D W L (\frac{8}{3\pi}\ Y_0 \omega_1)\dot{y}$$

where $\omega_1 Y_0$ is the maximum velocity of $\dot{y}$. If this approach is applied to pitch and roll the following equations result:

$$\text{Drag (heave)} = \frac{4.0\rho C_D LWY_0\omega_1\dot{y}}{3\pi}$$

$$\text{Drag (pitch)} = \frac{\rho C_D L^4 W\theta_0\omega_1\dot{\theta}}{24\pi}$$

$$\text{Drag (roll)} = \frac{\rho C_D W^4 L\phi_0\omega_2\dot{\phi}}{24\pi}$$

To check the validity of this linearization approach as well as the accuracy of the 64 element method, a comparison was made with values obtained from the exact drag equations shown in Figure 10. Since these exact equations are only valid for cases where single velocity terms are used, the comparison was done for a case where heave drag is only a function of heave velocity, pitch drag is only a function of pitch angular velocity, and roll drag is only a function of roll angular velocity. In other words, simple roll, pitch, and heave drag were tested independently.

The results of the comparison shown in Figure 11 indicate clearly how the finite element method compares almost identically with the exact values as computed with the equations of Figure 10. The one difference, that being that the linear approximation gave lower peak values as they appeared more sinusoidal in shape was anticipated because we are equating energy dissipation rather than peak values.

Additionally, to assure that the one term approximation will give the desired drag force at the proper time, a comparison was done between actual and linear drag values which would be created during normal cradle oscillations. Figures 12 through 14 compare drag values with Lulu exhibiting a

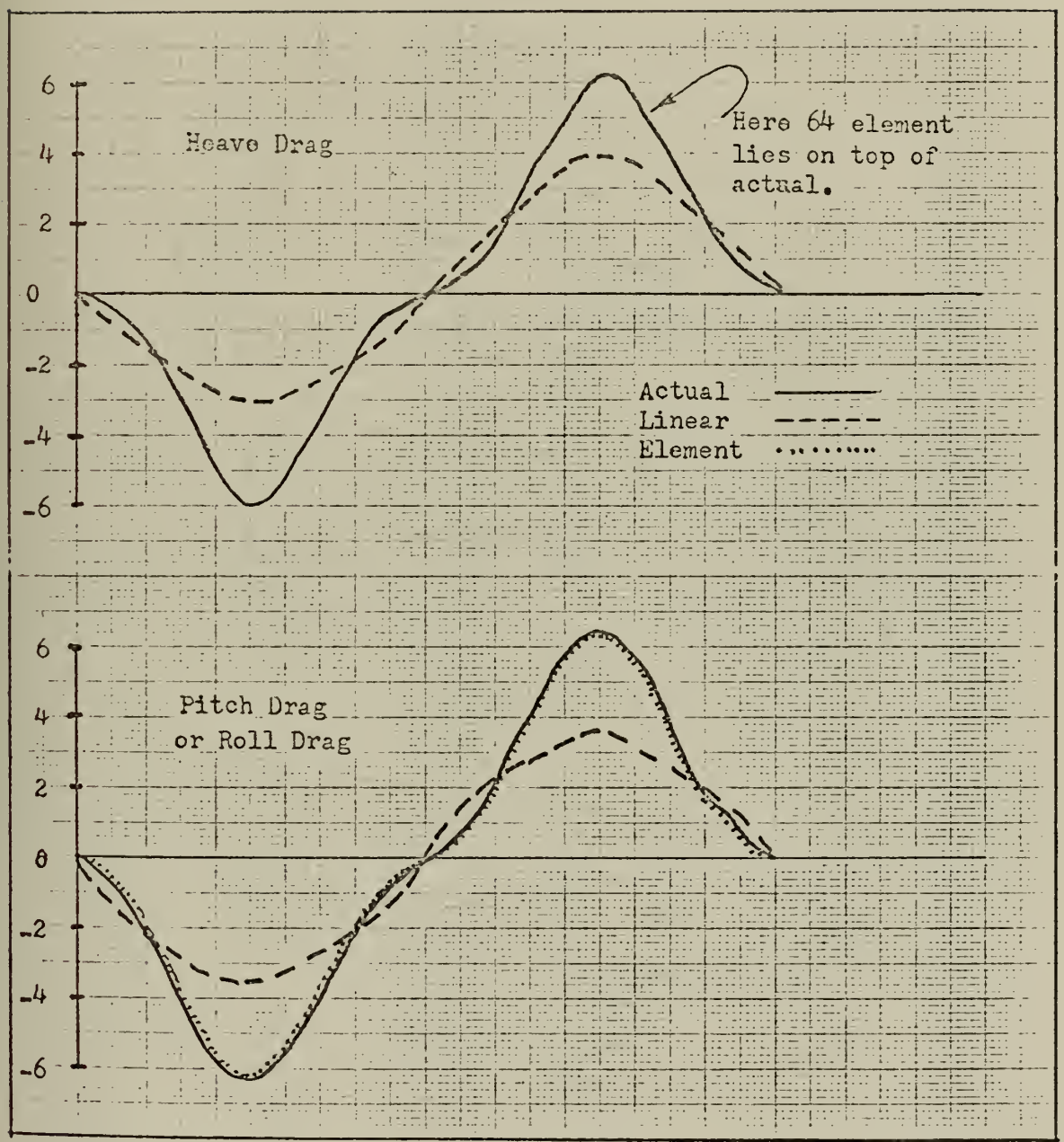
6
4
2
0
-2
-4
-6
Heave Drag
Here 64 element lies on top of actual.
Actual
Linear
Element
6
4
2
0
-2
-4
-6
Pitch Drag or Roll Drag

Figure 11.

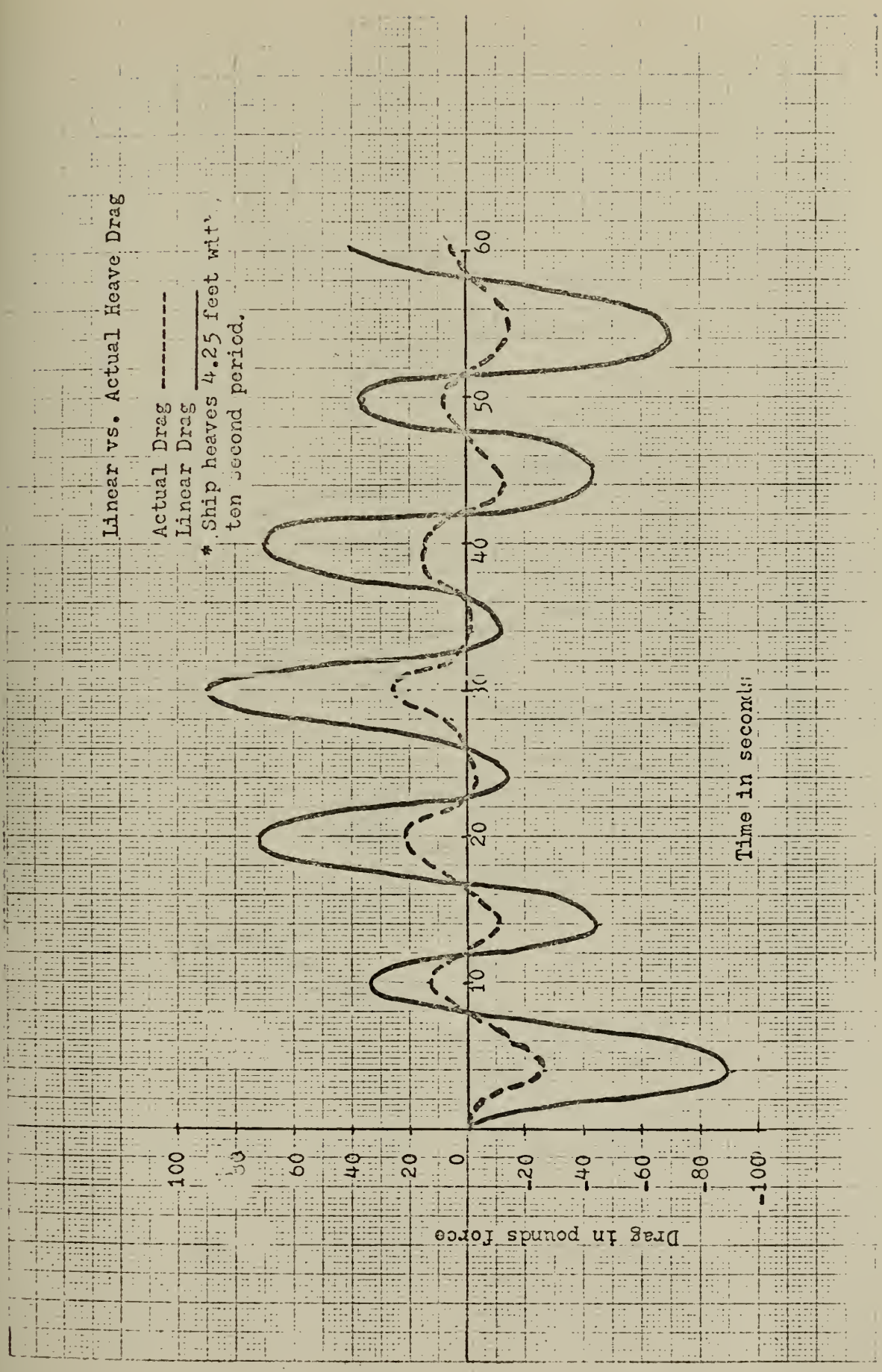
Linear vs. Actual Heave Drag
Actual Drag ---------
Linear Drag ———
* Ship heaves 4.25 feet with a ten second period.
Drag in pounds force
100
80
60
40
20
0
-20
-40
-60
-80
-100
10
20
30
40
50
60
Time in seconds

Figure 12.

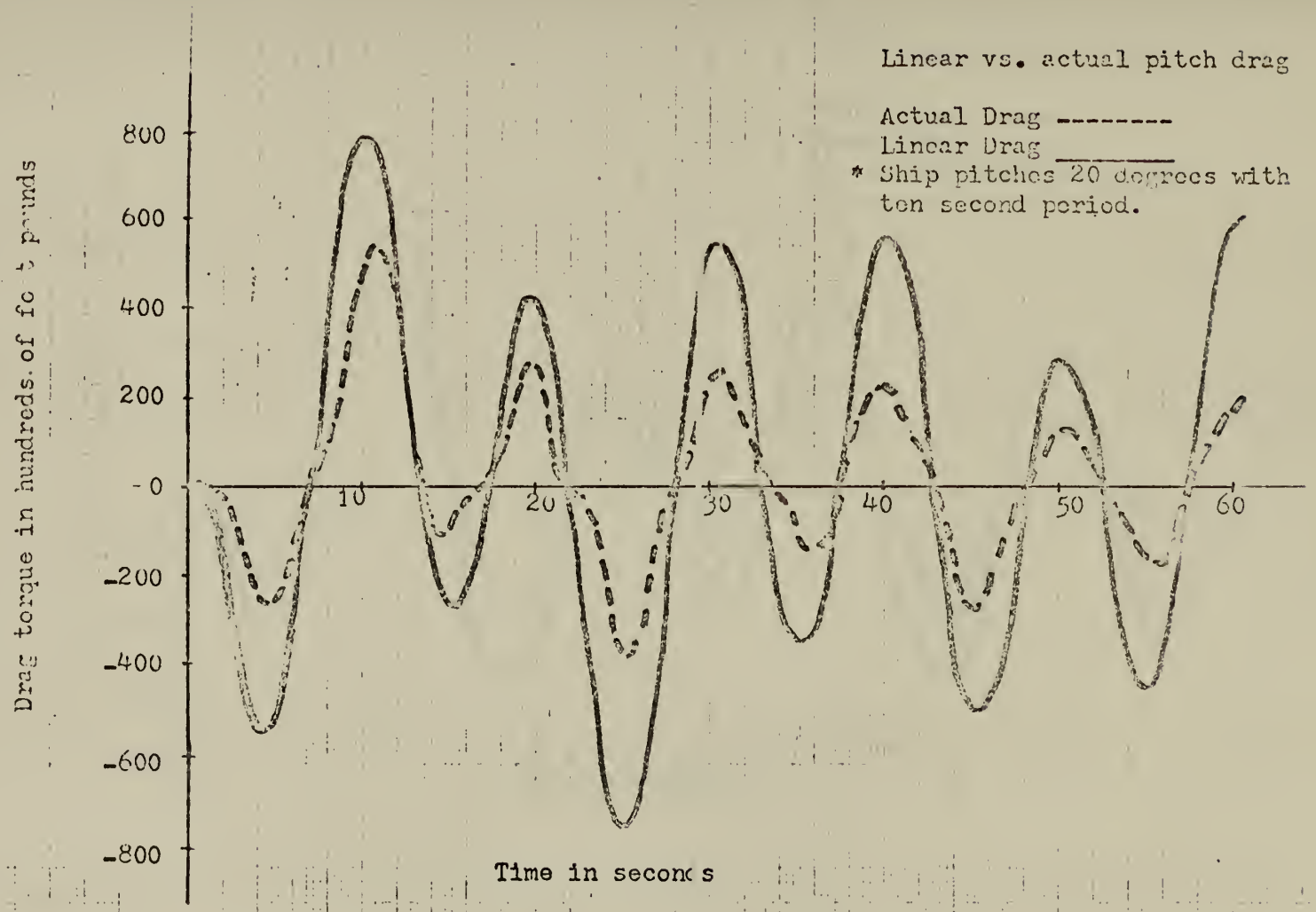
Linear vs. actual pitch drag
Actual Drag --------
Linear Drag ________
* Ship pitches 20 degrees with ten second period.
Drag torque in hundreds of foot pounds
800
600
400
200
-0
-200
-400
-600
-800
10
20
30
40
50
60
Time in seconds

Figure 13.

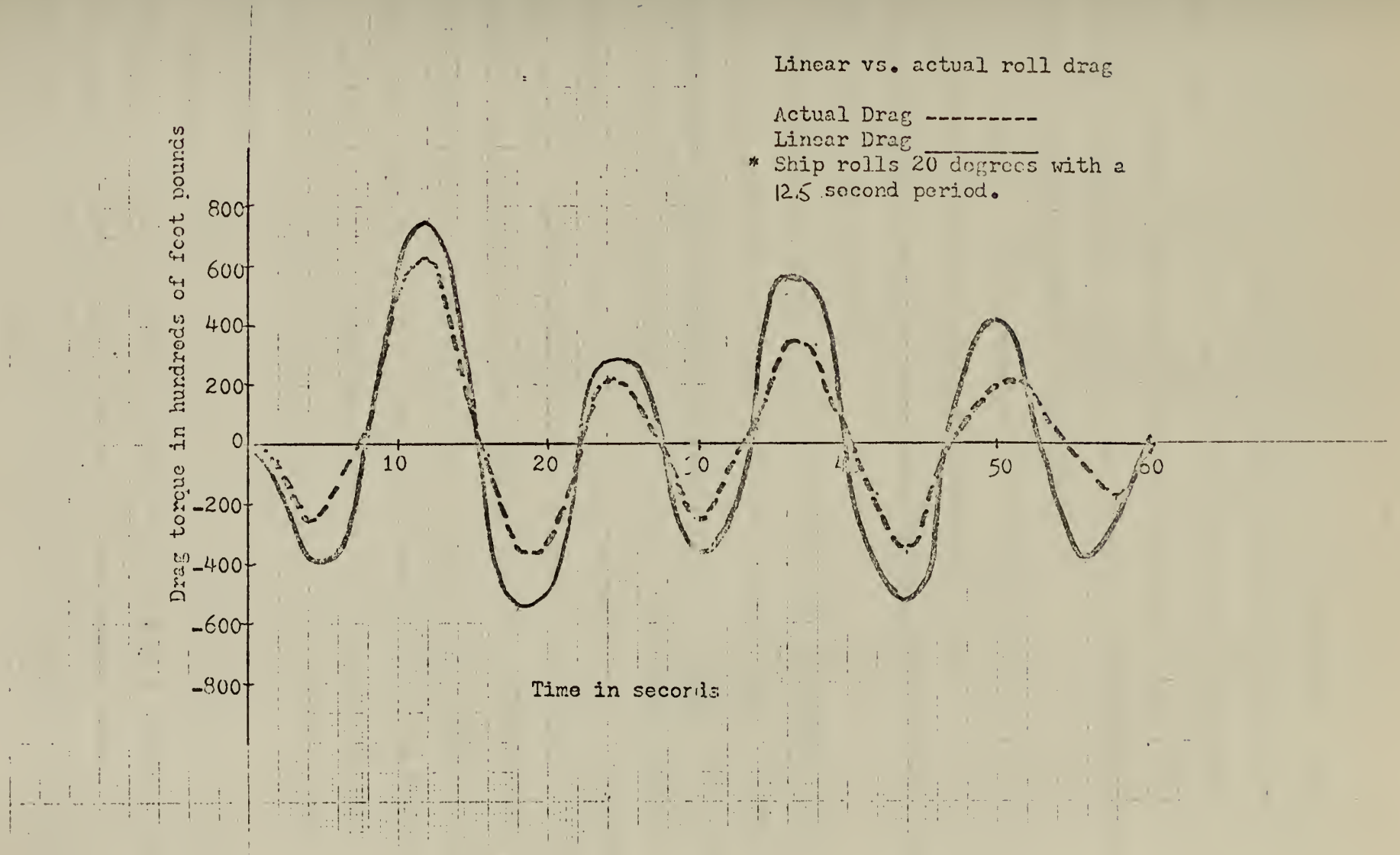
Linear vs. actual roll drag
Actual Drag ---------
Linear Drag _____
* Ship rolls 20 degrees with a 12.5 second period.
Drag torque in hundreds of foot pounds
800
600
400
200
0
-200
-400
-600
-800
10
20
50
60
Time in seconds

Figure 14.

ten second 20° roll and pitch, and a 4.25 ft. heave amplitude. The comparison shows that for this particular driving frequency and amplitude the linear approximation is in phase with the actual values, yet the amplitudes do not correspond. Another comparison at twice the frequency of the first confirmed that while a single variable drag term approximates the timing of the drag force well, it does not predict the amplitude.

In an attempt to better estimate the drag forces several two and three term approximations were investigated but the results showed that, in general, complete confusion reigned. Even worse, the drag forces were no longer in phase with the actual values.

The incorrect drag amplitudes result mainly from the terms in the coefficient of proportion of the linear drag term. In particular, for heave drag the constant $\frac{8}{3\pi}\omega_1 Y_0$, depends heavily on ω_1, the frequency of the cradle, and Y_0, the maximum displacement of the cradle. The cradle frequency ω_1 can be assumed to be the same as the driving frequency, but Y_0, the maximum cradle amplitude, cannot be assumed to be the same as the maximum driving amplitude. In actuality, Y_0 of the cradle is the maximum displacement of the cradle as given by the equations of motion. However, that value of Y_0 depends on the chosen value for the drag term, which in turn is a function of Y_0. Basically we have an iterative problem where values for the drag terms must be initially assumed and comparisons must be made with the actual nonlinear responses.

To provide a baseline for comparison a brute force analysis was conducted on the nonlinear equations to determine the actual response or gain of the system at various input frequencies. Ten separate frequencies were analyzed and the steady state gains were plotted versus frequency. The same

analysis was repeated but this time using the single term linear drag approximations in place of the accepted 64 element drag values. This analysis was also conducted at the ten different driving frequencies with three different driving amplitudes.

Figures 15 and 16 show clearly the differences between the linear and nonlinear responses at various driving frequencies. The roll response curve is ommitted since it falls just short of being on top of the pitch curves. These figures show that the linear approximations peak at the same frequencies as do the actual response curves but the gains vary widely depending on the input amplitude. In general, the linearized response curves show a condition of lesser damping than is actually the case. However, as the driving amplitudes go up, the apparent damping increases due to the presence of the larger value of driving amplitude (Y_0) in the coefficient of proportion.

Since the main value of such an analysis is the prediction of the resonance peaks, and since the linear and nonlinear responses are almost identical except in the range $0.5 \frac{\omega}{\omega_n}$ to $2.0 \frac{\omega}{\omega_n}$, it is valuable to correct the linear response curves by increasing the apparent damping until the linear responses conform to the nonlinear responses. This can be done by multiplying the previously discussed linearized drag terms by a constant depending on the magnitude of the driving amplitude.

Comparing the linear response curves to the simple single degree of freedom system shown in Figure 17, we find that the gain of such a system at resonance is given by the equation $\frac{1}{2\frac{C}{C_c}}$ where $\frac{C}{C_c}$ is the damping factor. Using this equation we find that the nonlinear heave resonance peak compares well to a linear system with a damping factor of 0.193. Similarly the pitch response compares well with a damping factor of 0.167. After finding the

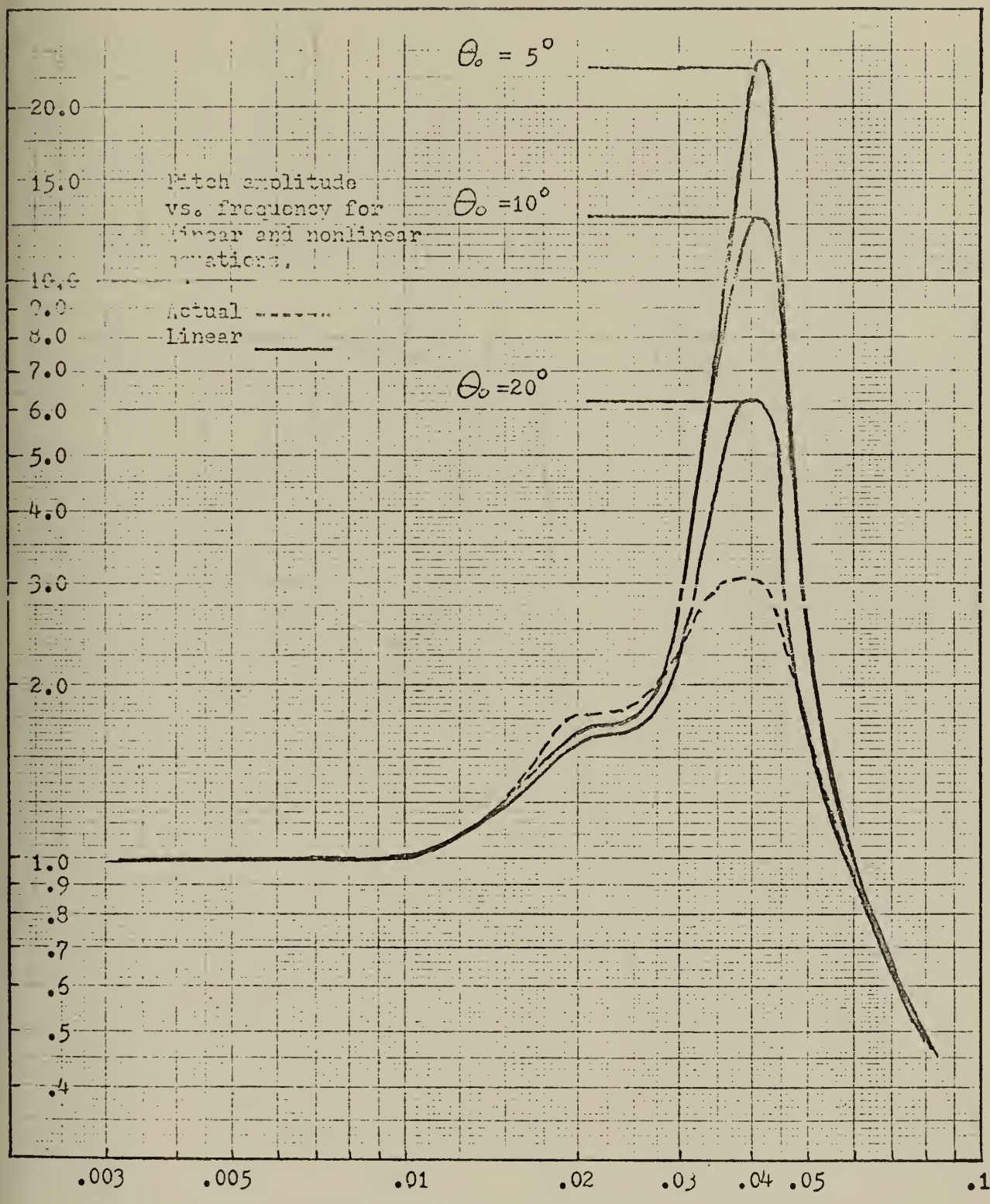

Driving frequency in Hertz

Figure 15.

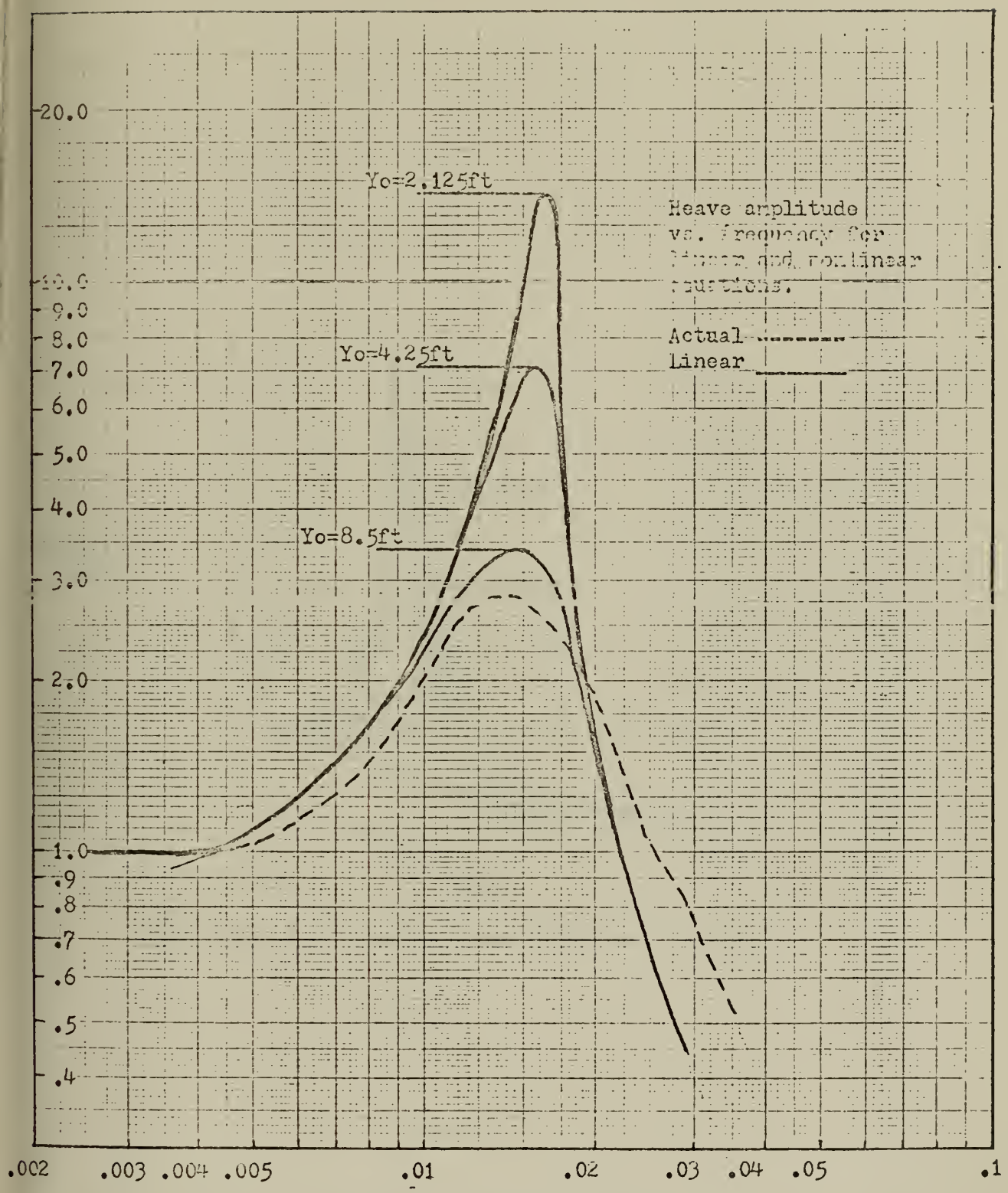
20.0
10.0
9.0
8.0
7.0
6.0
5.0
4.0
3.0
2.0
1.0
.9
.8
.7
.6
.5
.4
Yo=2.125ft
Yo=4.25ft
Yo=8.5ft
Heave amplitude vs. frequency for linear and nonlinear equations.
Actual
Linear
.002
.003
.004
.005
.01
.02
.03
.04
.05
.1
Driving frequency in Hertz

Figure 16.

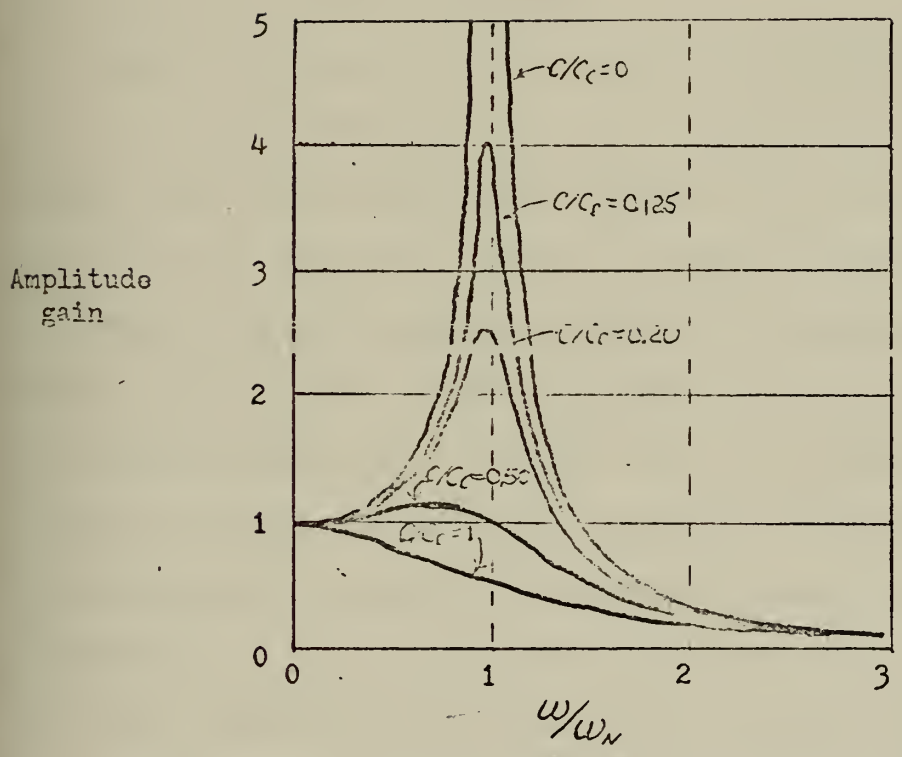

Single degree of freedom forced vibration response.

Figure 17.

indicated linear values of damping factors for the linear response curves with various input amplitudes, a plot of drag multipliers versus amplitude input was made. This plot, shown in Figure 18, indicates the factor by which the drag terms must be multiplied in order to make the linear response correspond closely to the nonlinear response for each input amplitude. For example, for our normal 4.25 ft. heave and 10° roll and pitch amplitude, the heave drag term would need to be multiplied by 2.7, the pitch drag term by 4.24, and the roll drag term by 4.0.

Summing up, linearization of the nonlinear drag terms is a complex matter. As in all problems in the physical sciences it is never feasible to express such linearizations with absolute certainty and with the inclusion of all possible variables. In fact, to treat any physical problem in a mathematical way it is necessary to first make assumptions about the system's behavior that may not be entirely correct. In this case drag is assumed to be linearly proportional to velocity, but, as is later discovered, it is also related to the driving amplitude and therefore appropriate correction factors must be applied. In spite of the difficulty involved, the value of this linearization is to provide the coefficients for the linear $\overline{A}$ matrix which can then be operated on to find the general trends of the system.

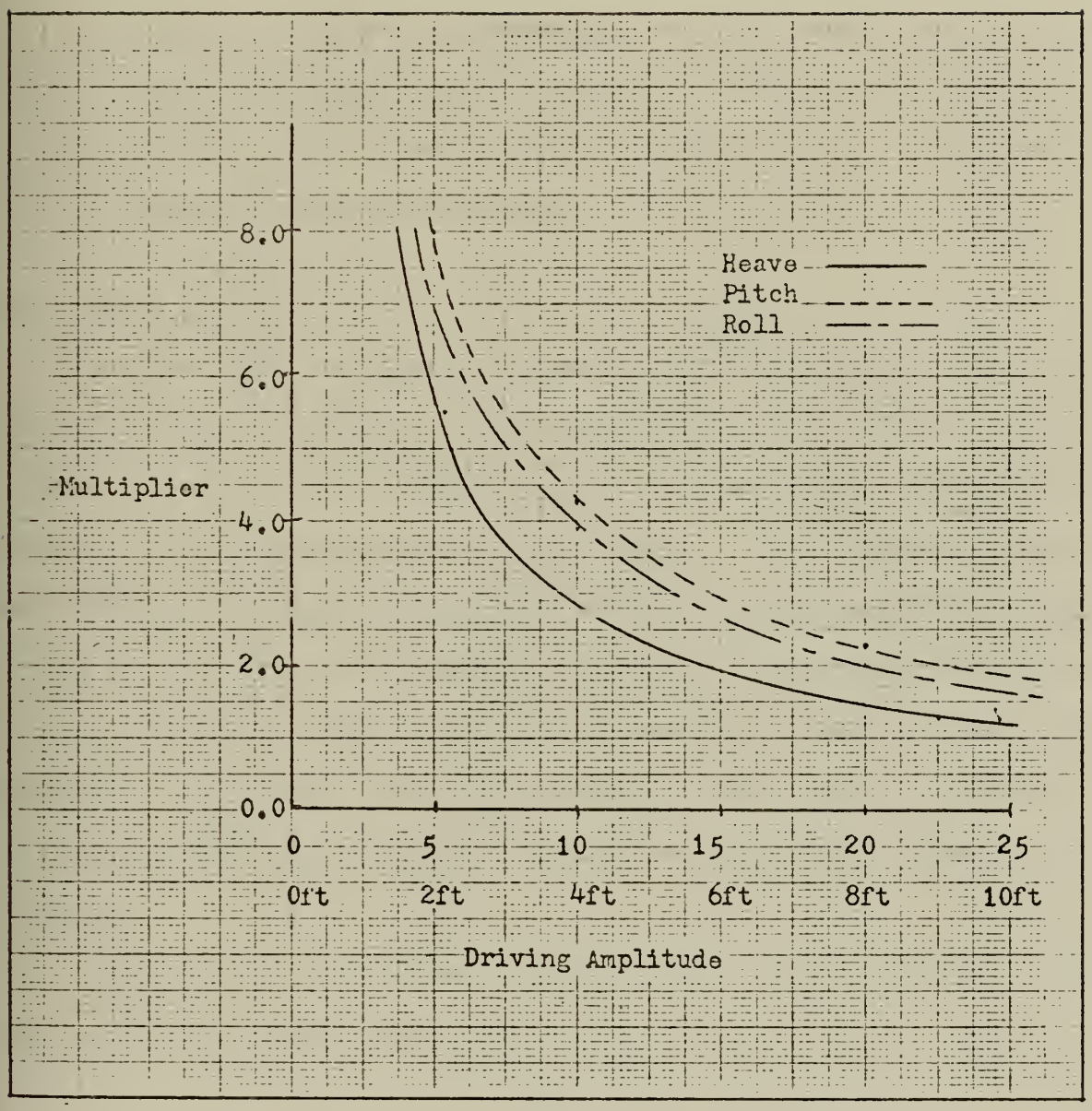
8.0
6.0
4.0
2.0
0.0
Multiplier
Heave
Pitch
Roll
0
5
10
15
20
25
0ft
2ft
4ft
6ft
8ft
10ft
Driving Amplitude

Figure 18.

CHAPTER IV.

SOLUTION OF EQUATIONS

The complete solution of differential equations may be split into two parts, a steady-state solution and a transient solution which dies out at a rate depending on the degree of damping, mass, and time. Our main interest here is with the steady-state solution.

Time Domain Analysis

The time domain solution of the equations of motion was found by the use of numerical integration. The integration was done using the newly installed Interdata computer facility at M.I.T.'s Mechanical Engineering Department. The same department's program DYSYS, (DYnamic SYstem Simulation), was used for the time domain analysis of the nonlinear equations. DYSYS solves a set of first order linear or nonlinear differential equations and can be particularly useful for obtaining transient as well as steady-state solutions to nonlinear time varying problems. DYSYS uses a fourth order Runge-Kutta integration technique to obtain an approximate solution to this equation--

Given Y_0, the value of the Y vector at some value of t, say t_0, then the approximate value of the y vector at $t_0 + \Delta t$ is

$$Y + \Delta t = Y_0 + \frac{\Delta t}{6}(K_0 + 2K_1 + 2K_2 + K_3),$$

the K's being equal to

$$K_0 = F(t_0, Y_0)$$

$$K_1 = F(t_0 + \frac{\Delta t}{2}, Y_0 + \tfrac{1}{2} K_0)$$

$$K_2 = F(t_0 + \frac{\Delta t}{2}, Y_0 + \tfrac{1}{2}K_1)$$

$$K_3 = F(t_0 + \Delta t, Y_0 + K_2)$$

The Runge-Kutta Method is derived from a Taylor Series Expansion about the point t_0 and Y_0. Theoretically, the method will converge to an exact solution as t approaches zero. The method has been shown to be stable, self-starting and to have a built-in error check.

Since the program is set up for simultaneous first order differential equations, the three second-order equations must be expressed as six first-order equations. This can be done by letting

$$y = y(1)$$

$$y(2) = \dot{y}(1) = \dot{y}$$

$$y(2) = \dot{y}$$

Similarly,

$$y(1) = \dot{y}$$

$$y(2) = \dot{y}$$

$$y(3) = \theta$$

$$y(4) = \dot{\theta}$$

$$y(5) = \phi$$

$$y(6) = \dot{\phi},$$

and hence y(1) through y(6) are the six state variables which completely define the system.

The computer program which was written to effect the solution is given in the appendix. The program has as subroutines EQSYM, which indicates "Equation Simulation" as well as three separate drag subroutines which must

be called each time step and calculates the drag at each point in the program. A time interval of 0.2 seconds was selected as a time step and gave reasonable results.

Frequency Domain Analysis

Since not only specific solutions for given parameters were desired, a frequency domain analysis resulting in Bode plots was undertaken. Bode plots clearly illustrate the relative stability of a system, with gain and phase margins often being defined in terms of Bode plots.

This analysis was conducted using the M.I.T. Mechanical Engineering Department computer program MBODE. This program calculates frequency domain gain and phase plots for linear dynamic systems (with constant coefficients) expressed in matrix form such as

$$\dot{x} = \overline{A}x + \overline{B}u$$

$$y = \overline{C}x + \overline{D}u$$

where

$\overline{A}$ = the system $\overline{A}$ matrix

$\overline{B}$ = the input matrix

$\overline{C}$ = the output matrix (usually diagonal ones or appropriate weighting factors)

$\overline{D}$ = the direct coupled output matrix (usually zero).

The fact that MBODE only operates on linear constant coefficient equations is the reason we were forced to develop linear approximations for the nonlinear drag terms discussed in section III. The Bode plots which

resulted from this method of analysis show clearly the properties of the system and these are presented in section V.

CHAPTER V.

DISCUSSION OF RESULTS

Time Domain Response

For this analysis numerous trials were run at various damping levels, input frequencies, input amplitudes, and spring constants. The majority of the trials were run at the baseline conditions of 4.25 ft. ship heave, 10° roll and pitch, and 20 $\frac{lbf}{ft}$ spring constant with a 10% deviation among the four springs. The 10% deviation is the method by which the nonideal nature of the springs was modeled and is the vehicle for energy transfer between the different motion modes.

In a discussion with J. Mavor of W.H.O.I. it was learned that the previously mentioned amplitudes with a 5-6 second period could be considered typical ship motions in a state four sea. Figure 19 shows this realistic situation of heave, pitch and roll and indicates that the transmitted ship heave is reduced from 4.25 ft. to about 5 inches while the roll and pitch are reduced from 10° to 2°. A total effective spring constant of 80-100 $\frac{lbf}{ft}$ is required to accomplish this decoupling; however, the analysis illustrates the fact that ship-cradle motion can be uncoupled if soft springs are used.

In Figure 20 the pitch and roll amplitude have been doubled and the ship has a slow 10-12 second period to give a "worst case" example of predicted cradle response. Although this decoupling is not as good as with the shorter period, the heave has still been reduced to less than one foot while the roll and pitch have been reduced from 20° to 10° and 7° respectively.

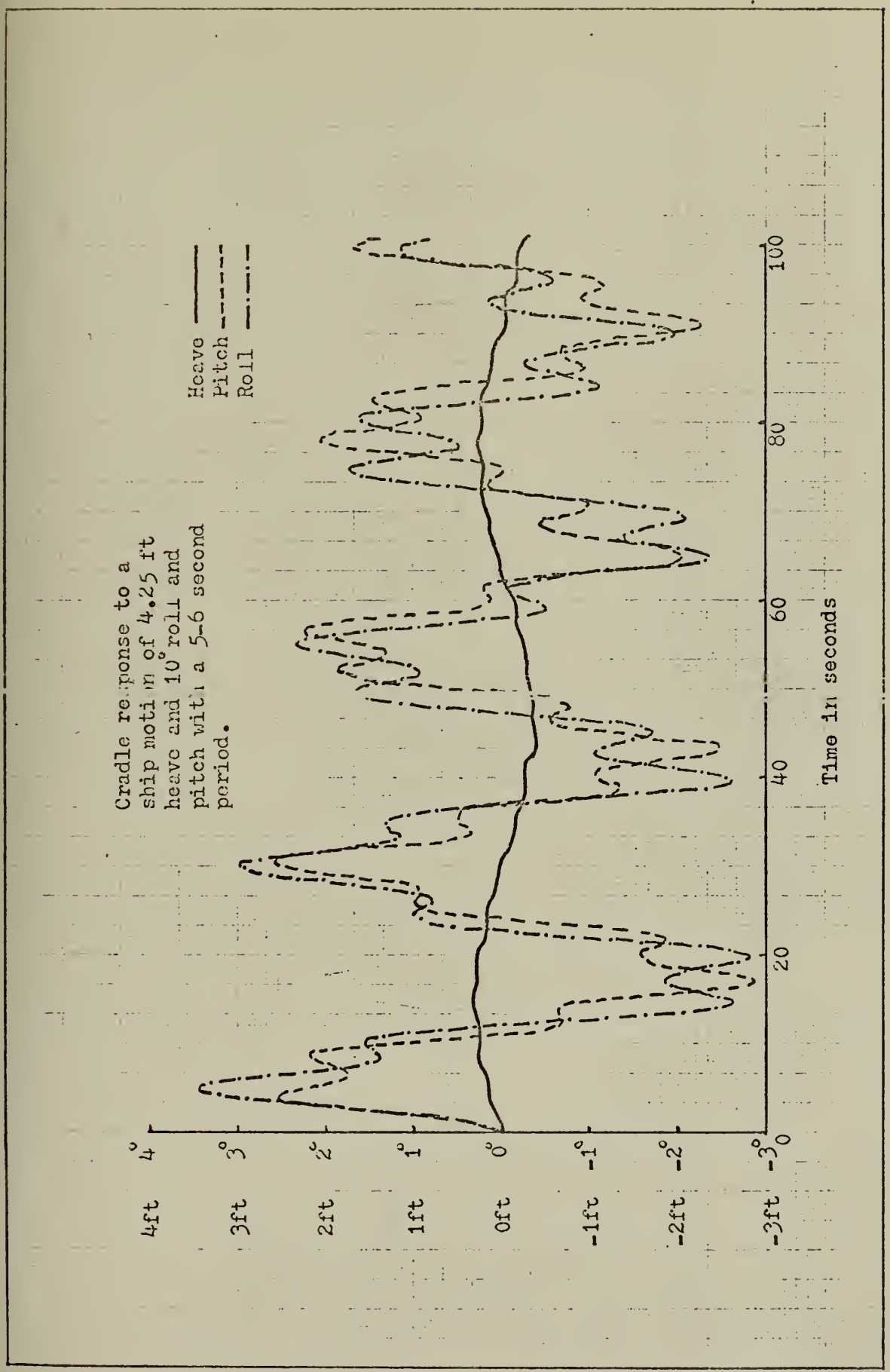
Cradle response to a ship motion of 4.25 ft heave and 10° roll and pitch with a 5-6 second period.
Heave
Pitch
Roll
4ft
3ft
2ft
1ft
0ft
-1ft
-2ft
-3ft
4°
3°
2°
1°
0°
-1°
-2°
-3°
0
20
40
60
80
100
Time in seconds

Figure 19.

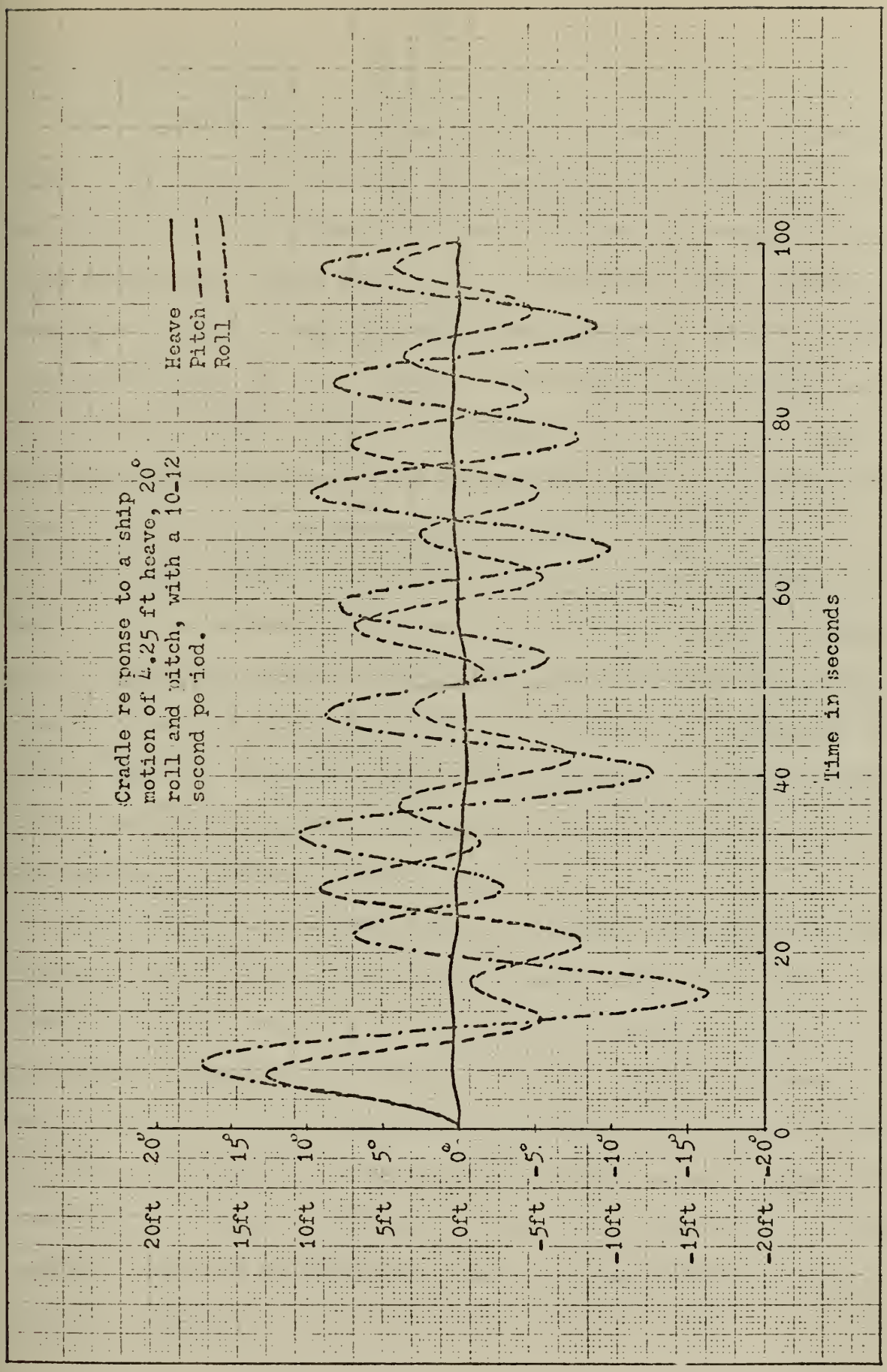
Cradle response to a ship motion of 4.25 ft heave, 20° roll and pitch, with a 10-12 second period.
Heave
Pitch
Roll
20ft
15ft
10ft
5ft
0ft
-5ft
-10ft
-15ft
-20ft
20°
15°
10°
5°
0°
-5°
-10°
-15°
-20°
0
20
40
60
80
100
Time in seconds

Figure 20.

Frequency Domain Response

Since specific response curves do not reveal much about the general nature of the system, a frequency domain analysis was conducted in order to get more descriptive information on how the system will react to various input frequencies. Figure 21 is a plot of the system's gain response at baseline conditions of amplitude and spring constant but at ten different input frequencies. It is, in effect, a Bode plot of the nonlinear case. The plot shows clearly the three reasonances of the system, the leftmost peak being the heave resonance and the rightmost peaks being pitch and roll resonances, the roll resonance being the smaller of the two.

This figure required ten separate solutions of the nonlinear equations of motion involving great expenditures of computer time. Although the plot shows the response of the system under fixed conditions of spring constant, mass, and driving amplitude, it is clearly not a desirable way in which to find how the system responds when differing sea conditions exist or when the system parameters are modified. It is here that the value of the linearization process comes into full view.

In Chapter III it was noted that the nonlinear drag terms could be linearized once the driving amplitude was known. Again using the 4.25 ft. heave with 10° roll and pitch as the baseline we can find the linear drag approximation by referring to Figure 18, Chapter III, and obtaining the proper multiplier. Once these drag coefficients are set, Bode plots may be initiated which show the response of all outputs versus all inputs over a wide frequency range. Additionally, the effects of variations in spring constant or mass may be studied with only minor modifications to the now linearized $\bar{A}$ matrix.

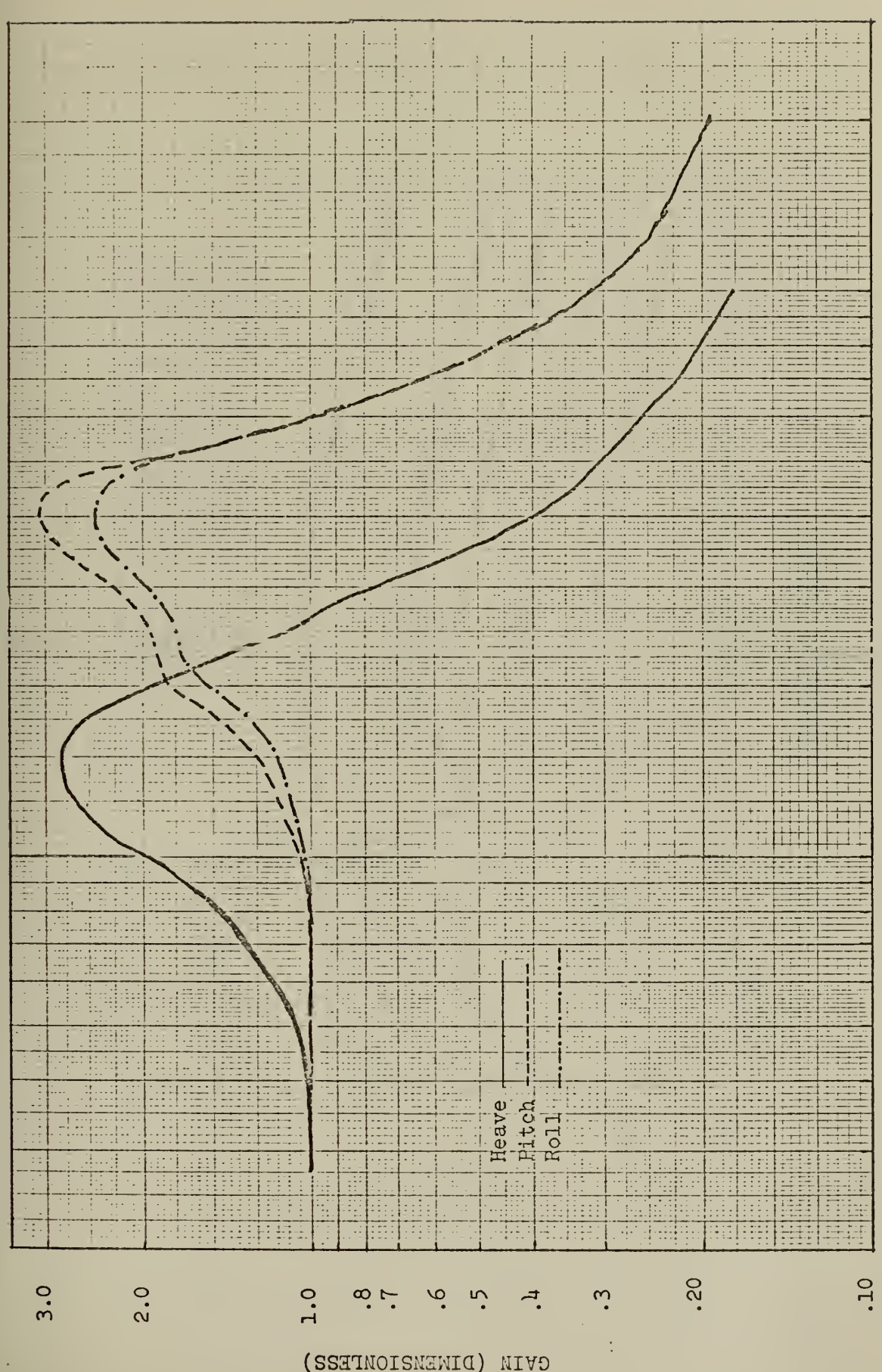
GAIN (DIMENSIONLESS)
3.0
2.0
1.0
.8
.7
.6
.5
.4
.3
.20
.10
Heave
Pitch
Roll
.002 .003 .004 .006 .008 .01 .02 .03 .04 .05 .06 .07 .08 .09 .10 .20 .30
DRIVING FREQUENCY IN HERTZ

Figure 21.

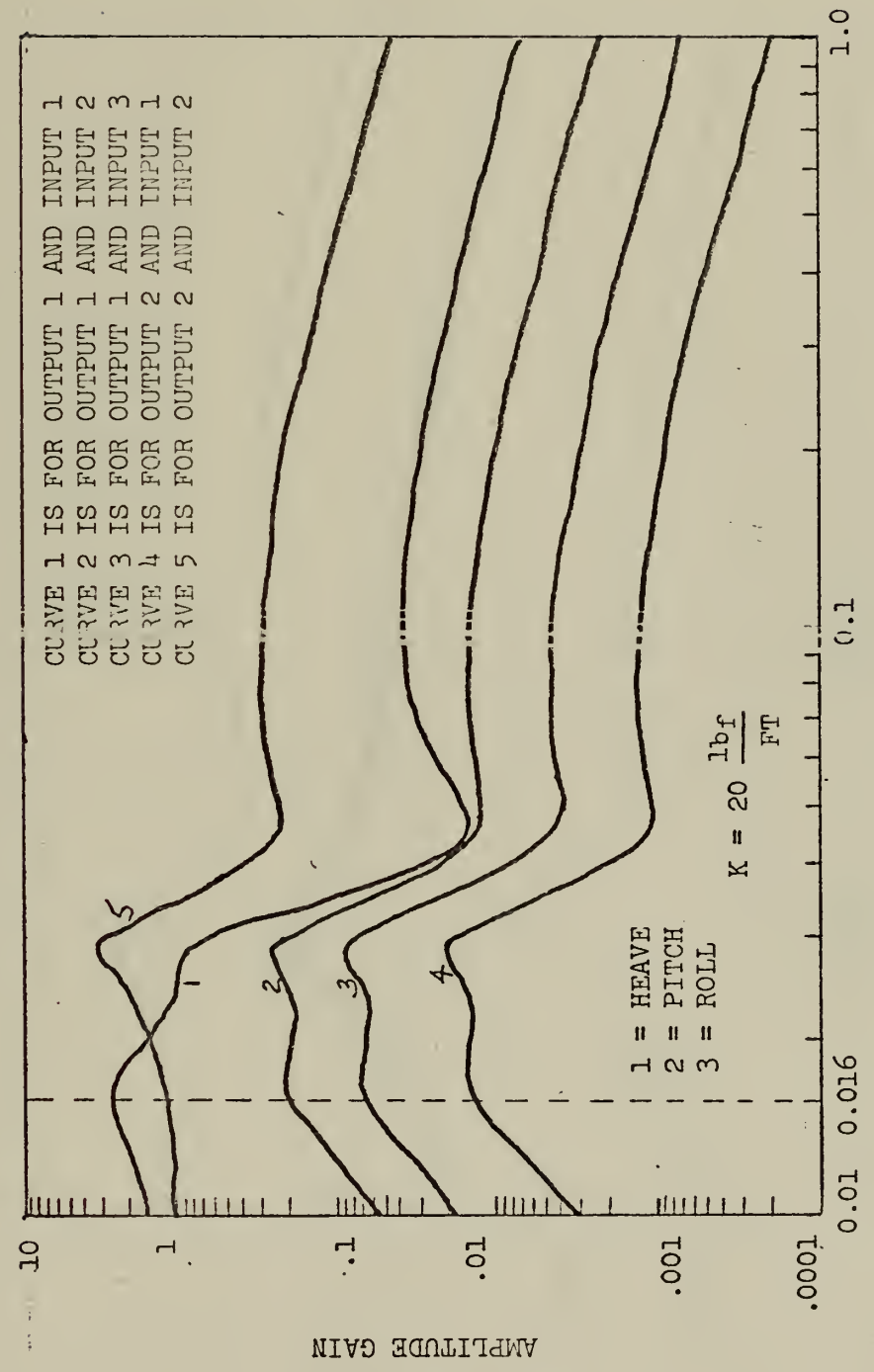
CURVE 1 IS FOR OUTPUT 1 AND INPUT 1
CURVE 2 IS FOR OUTPUT 1 AND INPUT 2
CURVE 3 IS FOR OUTPUT 1 AND INPUT 3
CURVE 4 IS FOR OUTPUT 2 AND INPUT 1
CURVE 5 IS FOR OUTPUT 2 AND INPUT 2
1 = HEAVE
2 = PITCH
3 = ROLL
K = 20 lbf/FT
AMPLITUDE GAIN
10
1
.1
.01
.001
.0001
0.01
0.016
0.1
1.0
FREQUENCY IN HERTZ

Figure 22.

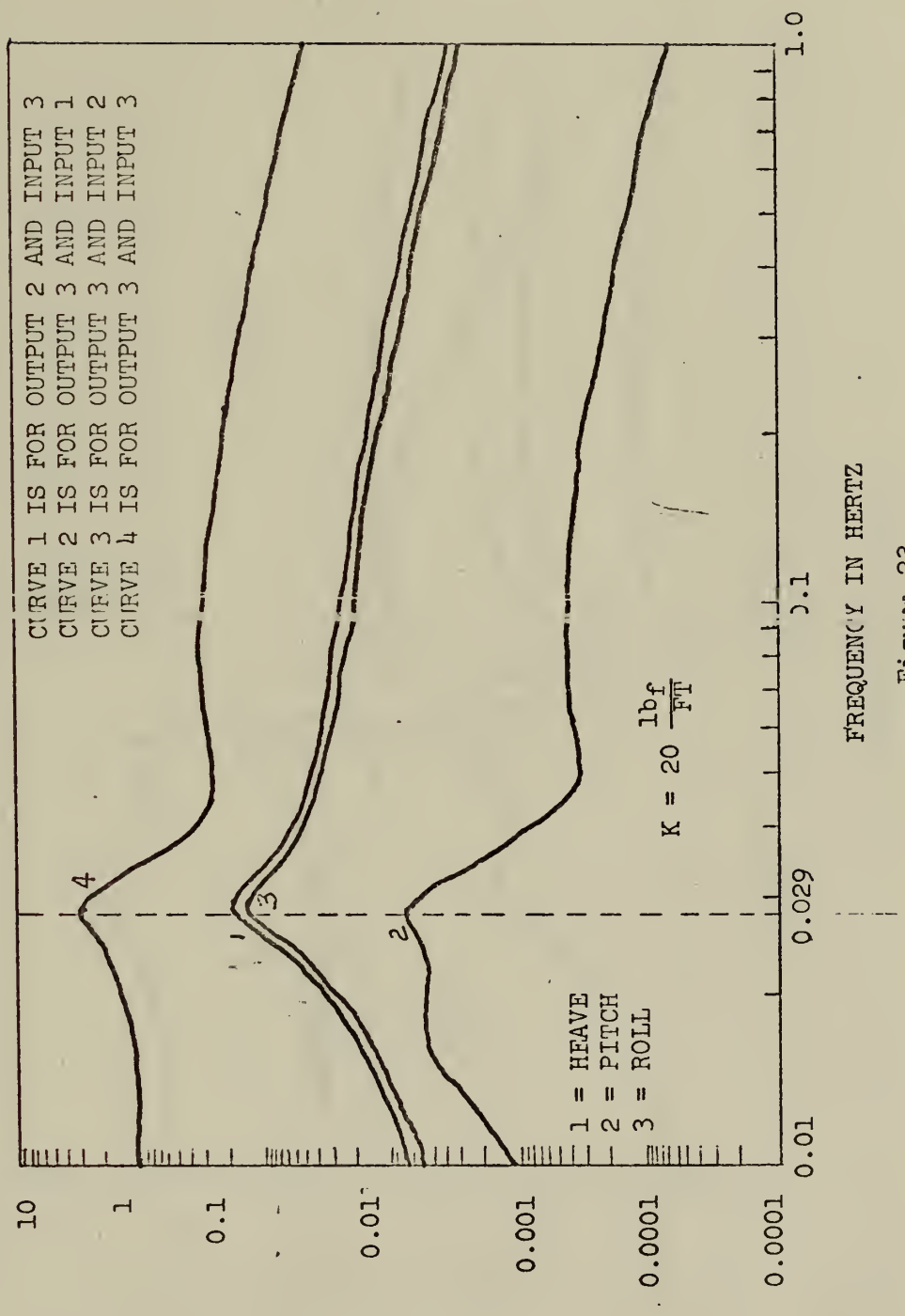
CURVE 1 IS FOR OUTPUT 2 AND INPUT 3
CURVE 2 IS FOR OUTPUT 3 AND INPUT 1
CURVE 3 IS FOR OUTPUT 3 AND INPUT 2
CURVE 4 IS FOR OUTPUT 3 AND INPUT 3
1 = HEAVE
2 = PITCH
3 = ROLL
K = 20 lbf/FT
AMPLITUDE GAIN
10
1
0.1
0.01
0.001
0.0001
0.01
0.029
0.1
1.0
FREQUENCY IN HERTZ

Figure 23.

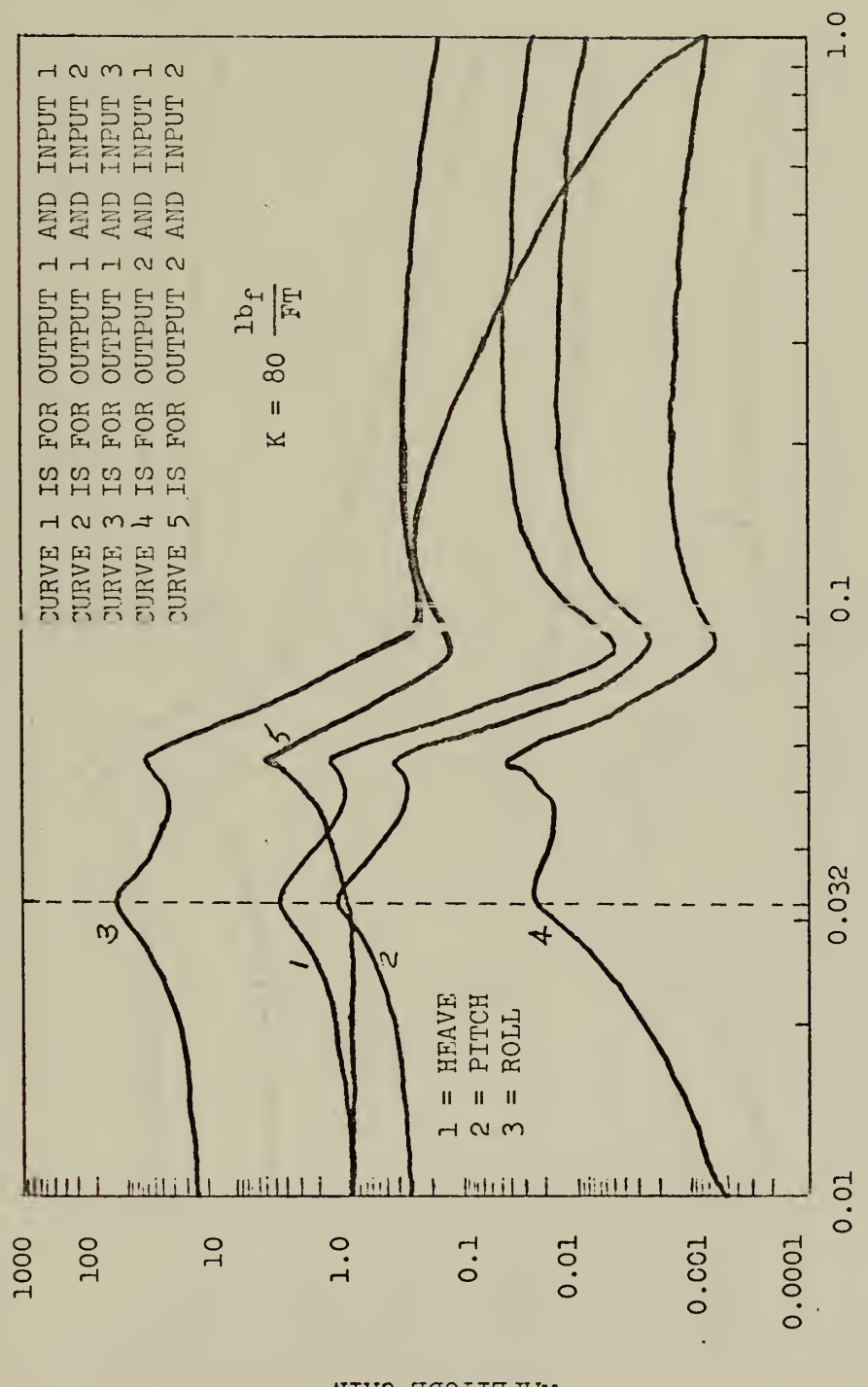
CURVE 1 IS FOR OUTPUT 1 AND INPUT 1
CURVE 2 IS FOR OUTPUT 1 AND INPUT 2
CURVE 3 IS FOR OUTPUT 1 AND INPUT 3
CURVE 4 IS FOR OUTPUT 2 AND INPUT 1
CURVE 5 IS FOR OUTPUT 2 AND INPUT 2
K = 80 lbf/FT
1 = HEAVE
2 = PITCH
3 = ROLL
AMPLITUDE GAIN
1000
100
10
1.0
0.1
0.01
0.001
0.0001
0.01
0.032
0.1
1.0
FREQUENCY IN HERTZ

Figure 24.

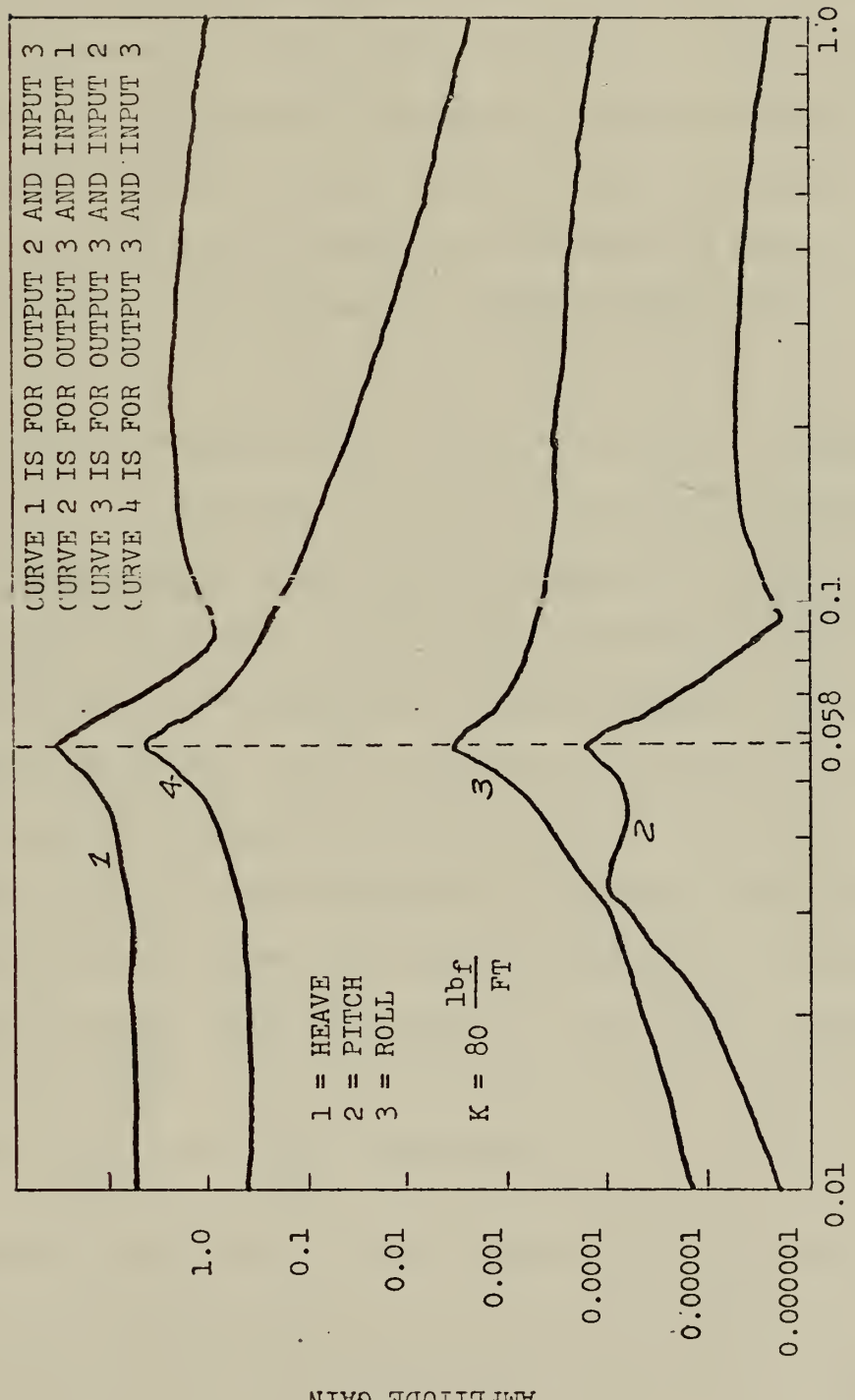
CURVE 1 IS FOR OUTPUT 2 AND INPUT 3
CURVE 2 IS FOR OUTPUT 3 AND INPUT 1
CURVE 3 IS FOR OUTPUT 3 AND INPUT 2
CURVE 4 IS FOR OUTPUT 3 AND INPUT 3
1 = HEAVE
2 = PITCH
3 = ROLL
K = 80 lbf/FT
1
2
3
4
AMPLITUDE GAIN
1.0
0.1
0.01
0.001
0.0001
0.00001
0.000001
0.01
0.058
0.1
1.0
FREQUENCY IN HERTZ

Figure 25.

Figures 22 through 25 show the system's response across a range of .01 to 1.0 Hertz or a roll pitch and heave period of 1.0 to 100.0 seconds. The outputs for heave versus ship pitch and roll show that the ship's pitching and rolling couples energy into heave motion which then peaks at heave natural frequency as well as the pitch and roll natural frequency. This fact indicates the dangers of designing a decoupling system to decouple only heave. It is clear from the plot that a decoupling system designed only for heave may well excite the pitch and roll modes at their natural frequencies. This fact was overlooked by single degree of freedom analysis.

Several other conclusions may be drawn from Figures 22 through 25. While a 20 lbf/ft was chosen as a baseline for the spring constants and was used for Figures 22 and 23, it would be desirable to predict easily what would happen with higher or lower spring constants. Figures 24 and 25 show the response of the system with a spring constant of four times that of Figures 22 and 23. It is not surprising to see that the resonant frequencies are shifted upward by a factor of approximately two. This indicates that in spite of the nonlinearity of the parent system, the system obeys the basic laws for calculating natural frequencies of translational and rotational systems. Being more specific, heave natural frequency is proportional to $\frac{\sqrt{Keff}}{Mt}$, while pitch and roll natural frequencies are proportional to $\frac{\sqrt{KL}}{I1}$ and $\frac{\sqrt{KL}}{I2}$ respectively.

As a result of the above, we have information on the system's behavior over a wide range of frequencies without the need of calculating a Bode plot for each value of K. In effect, using K = 20 lbf/ft as the starting point,

we need only shift the response peaks up or down the frequency scale by a factor of the square root of K_{new}/K_{20}, or $\frac{\omega_{new}}{\omega_{old}} = W_{old} \sqrt{\frac{K_{new}}{K_{20}}}$.

This same method of peak shifting can be applied to variations of mass or moment of inertia in a like manner, but in this case the shift will be proportional to $\frac{\sqrt{Mt(base)}}{Mt(new)}$ or $\frac{\sqrt{I(base)}}{I(new)}$.

Summing up, this analysis has shown that motions of a submerged cradle can, in fact, be nearly decoupled from surface ship motions if a soft effective spring constant is provided at the four cradle corners. In addition, the analysis has shown that the critical design consideration is the pitch and roll natural frequency rather than the natural frequency of heave. As a result, careful thought must be given to the selection of spring constants since the equations of motion are coupled and are capable of transferring energy from one mode to another and hence exciting other modes at their natural frequencies.

CHAPTER VI.

APPLICATION POSSIBILITIES

It is not the major objective of this thesis to offer a detailed design of a decoupling system. It is enlightening, however, to discuss several approaches that could be applied in the design of such a system. The primary consideration here is to obtain a soft spring constant and still support a large static load.

From the previous analysis it is apparent that the soft spring constant must be at the four cradle corners. Further review indicates a spring constant between 20 and 50 lb_f/ft would seem to be a reasonable selection for these corner springs.

At this point there are two types of approaches to consider. The first and simplest approach is the passive system where we try to create a spring with the proper softness so that without any outside control the springs will decouple the ship-cradle motions. This approach can be likened to vibration isolation of a motor or a vibrating mass. It is simple and reasonably foolproof.

The alternative method is of course a more complex active system where some sort of control is used to actively uncouple the two motions. This control can be in the form of position, velocity, acceleration, integral or differential feedback, horizontal sensing transducers or mechanical linkages. Consequently, unlike passive systems, these types of systems can be tuned to changing sea conditions or conditions of loading, thereby giving them a possible advantage.

Passive Systems

To create a passive system for the cradle would require consideration of several methods of achieving the desired soft spring constant. A first choice for component selection would probably be simple metallic springs which deform in accordance with Hooke's Law. Unfortunately, the static cradle weight of about 16,000 pounds would stretch the four 50 lb_f/ft springs to about 80 feet before reaching equilibrium. Clearly, this would be unacceptable for if coil springs were used they would necessarily resemble long "slinkys" and would prove completely unmanageable. Leaf springs would similarly be of little use as they too would deflect excessively in the static mode.

Torsional springs would possibly work if they were rigged through a complex gearing system which wound up as load was applied; however, they too would require a large static deflection under the simple cradle load and would involve complex machinery and cable drums. Such a mechanical system would probably be more of a liability than an asset in an ocean environment.

Another possible alternative might be to take advantage of the non-linear stress strain properties of elastomers. Vulcanized rubber will stretch to nearly ten times its own length and support up to ten tons per square inch. Unfortunately, the resistance to deformation usually increases in greater proportion than does the extension. If, by special treatment, an elastomer with the opposite properties were developed, it might be a logical choice to use as a spring. However, a short literature search turned up no suggestion that such a material exists.

A more reasonable method of producing such an effective spring constant would be with a hydraulic or pneumatic device. A device such as a hydraulic or pneumatic cylinder has the advantage that it can be biased to an initial static load and then oscillate about that equilibrium position with an effective spring constant which depends on pressure, temperature, properties of the fluid, and dimensions of the system.

To illustrate such a system consider Figure 26.

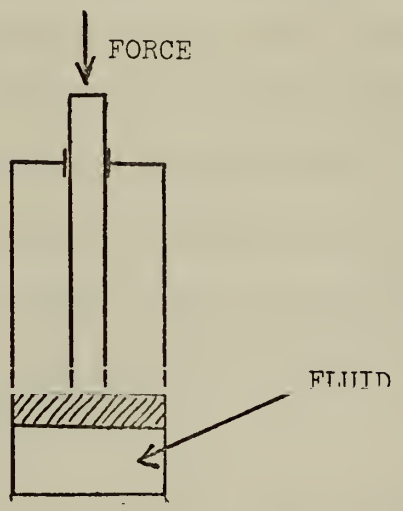

Figure 26.

This system would have a spring constant which would depend heavily on κ, the compressibility of the fluid. It is evident that a fluid with a high compressibility, such as air, would result in a softer overall spring constant which is desirable in this case. Additionally, a decoupling system with air springs would be capable of being set to an initial static force equal to that of the cradle weight. This might be accomplished with a simple pressure regulating device. Following initial set, the cradle could then oscillate about equilibrium with a soft effective spring constant depending on the previously mentioned parameters.

Before considering this simple approach there are two important considerations to be aware of. First, the oscillating piston must look exactly like a soft spring to the disturbing ship motion. That is, the difference in piston force from equilibrium to the extremes of piston travel must compare well with what would be seen if a real metallic spring were being used. In other words, for a ten foot pneumatic cylinder with a normally centered piston (capable of ± 5 foot excursions), the fully extended piston force must be equal to static cradle weight plus K (effective) · 5 feet. For example, if the desired spring constant were 50 lb_f/ft, then the piston could only exert 250 lb_f more than the cradle weight at its maximum stroke of five feet. Quickly calculating the change in pressure for full compression using $P_1V_1 = P_2V_2$, it is obvious that if the pneumatic system were dead ended, the reduction in volume to 1/5 of its previous value would result in a fivefold increase in pressure.

Consequently, the first consideration in such a design is the fact that a plenum chamber would have to be used in conjunction with such a system in order to have the desired results. To illustrate the size of the required plenum chamber, we can again use $P_1V_1 = P_2V_2$ (if $T_1 = T_2$). Assuming a baseline piston area of 1 $ft.^2$, a static cradle load of 4000 lb_f per spring would require a piston pressure difference of 278 psi in order to maintain the cradle at equilibrium. Calculating the plenum size required with the following conditions

$$\Delta V \text{ at full stroke} = 5 \text{ ft.}^3$$

$$\Delta F \text{ at full stroke} = 250 \text{ lb}_f$$

$$P_1V_1 = P_2V_2 \quad \text{or} \quad 278\ V_1 = (278 + 1.7)\ (V_1 - 5 \text{ ft}^3)$$

$$V_1 = 815 \text{ ft}^3$$

we unfortunately find it is a chamber far exceeding the capacity of the cradle to easily carry.

However, further calculations show that the size of the required plenum will go down as working pressure goes up. For example,

assume $P_1 = 2000$ psi

Piston area = 2 in.^{2}

or $2000\ V_1 = (2000 + 125)\ (V_1 - .069)$

$V_1 = 9.4$ ft.^{3}

and is a volume which is well within the carrying capacity of the cradle.

The second major consideration in passive system design is the problem of centering the system. With a pneumatic spring such as is sketched in Figure 27, the piston and plenum might be pressurized on the surface until the piston was positioned at midstroke and supporting the cradle's weight.

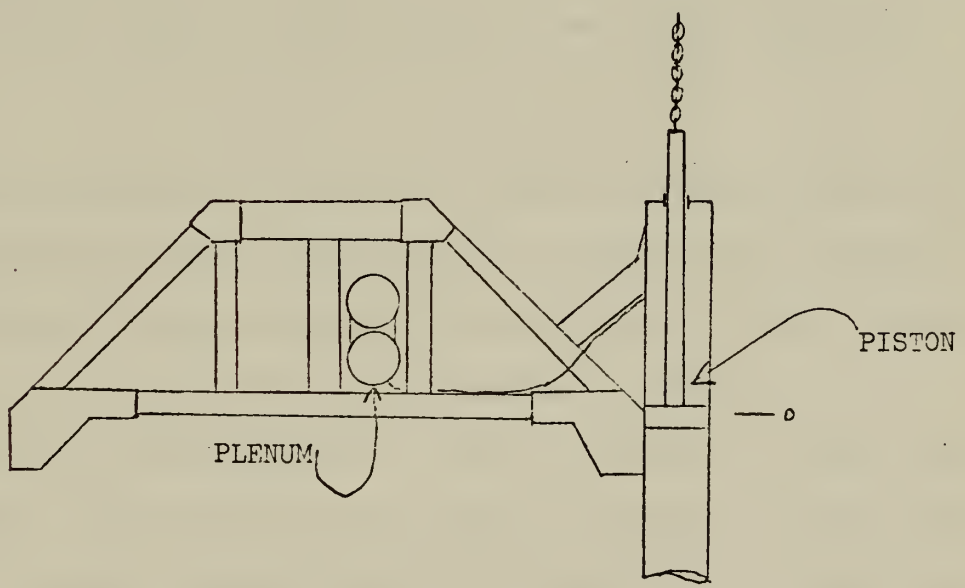

Figure 27.

This initial setting, although correct on the surface, would be incorrect after the effects of hydrostatic pressure, temperature, and leakage had taken place. This fact would necessitate the constant bleeding in of make-up gas. In effect, some active control would be necessary to make this passive design workable.

In addition to the aforementioned major design considerations, when using a gas, with its higher compressibility, there are serious technical problems to be overcome. These problems involve containment of a gas under high pressure, sealing, and danger of explosion, all of which may lead to bulky and expensive design.

Throughout this entire first section only passive decoupling systems are discussed. These systems all have the same characteristics in that they oscillate about an equilibrium position not determined actively by sensors and feedback, but by cradle weight, system dimensions, and initial conditions.

Active Systems

Systems which employ active feedback for control are called active systems. Typical examples of these systems include automobile power steering, hydraulic positioning devices, and automated milling machine tables. These active systems are all characterized by a mechanical, electrical, or hydraulic system by which information on the output is fed back to control the actions of the input. This feedback control can be designed to provide fast or slow response, maximum or minimum overshoot or undershoot, and nearly any natural frequency within the constraints imposed by the parameters of the system.

The simplest form of an electrohydraulic position control device is

shown below in Figure 28.

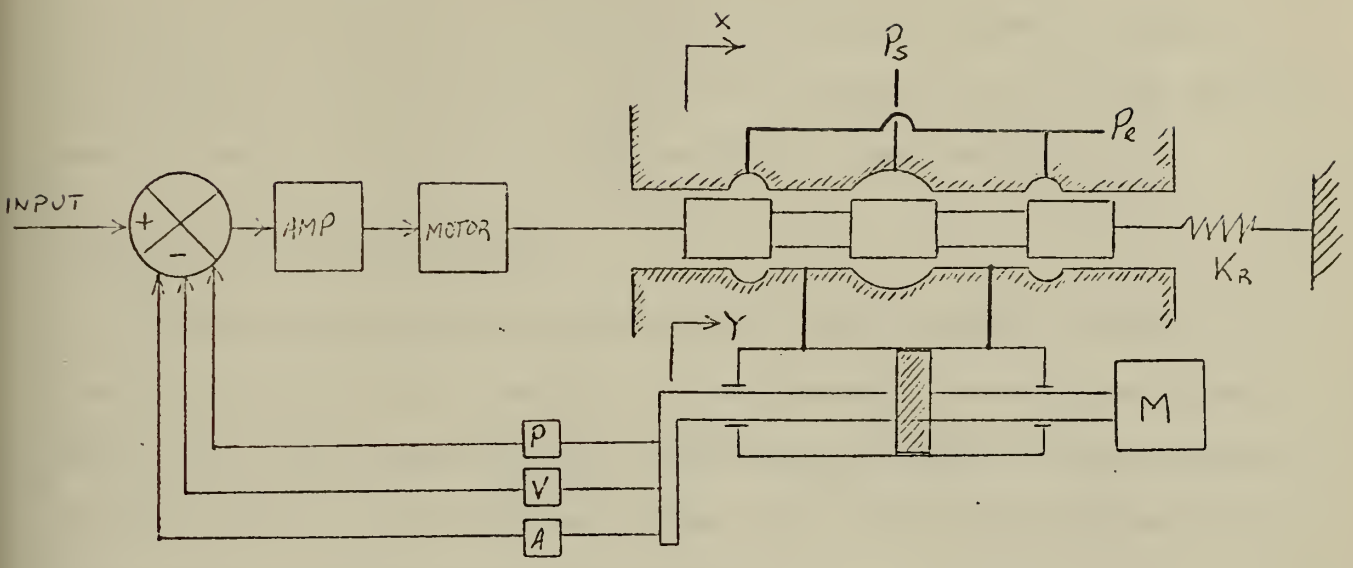

Figure 28.

The feedback loop consists of sensors which feed back position, velocity, and acceleration information which improve the system's response to disturbances at the input. Position feedback often is sufficient for system control but does not provide the tight feedback loop that results when velocity and acceleration are also used.

A typical response curve for such a system is shown in Figure 29.

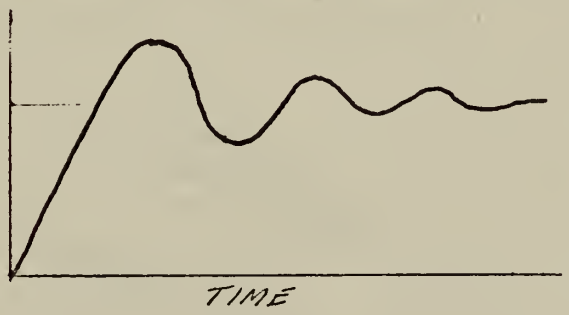

Figure 29.

That is, the system would tend to rise to the desired level, overshoot it, and then oscillate about that level with a decaying oscillation depending on the parameters of the system. It is this oscillation which might well be used to create a virtual soft spring constant at the constant load.

A Proportional Control Approach

As previously stated, feeding back all three variables would tend to make the system have less overshoot and oscillation. Since we are attempting to utilize the system's natural oscillations, we would be more successful using only a position feedback system which, while not enhancing oscillations, does not discourage them strongly.

To determine the feasibility of such a system and to get some design parameters for guidance, the system equations are determined below.

First, looking at the spool valve and assuming the hydraulic fluid is water,

Valve flow--

$$Q_m = K_{ox} X - K_{op} P_m$$

where Q_m = flow to load

K_{ox} = flow sensitivity or valve gain

K_{op} = negative slope of valve characteristic curve at constant value of x. See Figure 30.

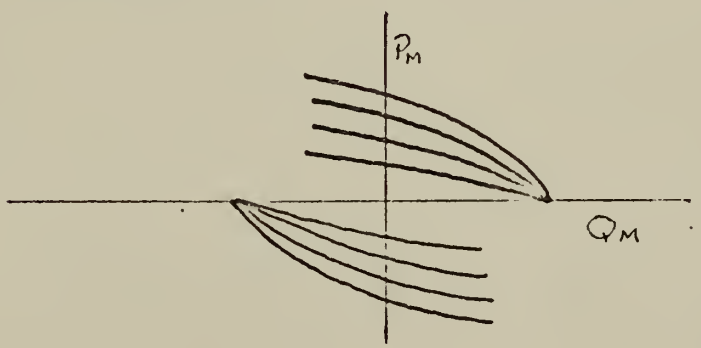

Figure 30.

For an ideal valve the slope, K_{op}, is very small and can be assumed as zero. Such a valve is called a flow control valve.

Valve forces--

$$-K_R X + F_i = 0$$

where K_R = valve control spring

F_i = valve force

Next, considering the piston,

Piston flow--

$$Q_m = A\dot{y} + \dot{P}_m \tfrac{1}{2} \left(K_e + \frac{V}{\beta_m}\right) + C_2 P_m$$

where:

C_2 = piston leakage

K_e = compliance of piston

V = volume of piston chamber

β_m = bulk modulus of fluid

Piston forces--

$$M\ddot{y} = P_m A + W_t$$

A = area of piston

M = mass of load

W_t = weight of static load

Combining all four equations,

$$K_{ox} X = A\dot{y} + \dot{P}_m \tfrac{1}{2}\left(K_e + \frac{V}{\beta_m}\right) + C_2 P_m$$

and: $M\ddot{y} = P_m A + W_t$.

Finally,

$$\frac{M\ddot{y}}{A}\left(\tfrac{1}{2}\left(K_e + \frac{V}{\beta_m}\right)\right) + \frac{C_2 M\ddot{y}}{A} + A\dot{y} = K_{ox} X$$

and using LaPlace transforms,

$$\bar{y}(s) = \frac{K_{ox}\bar{X}(s)}{s(s^2\frac{M}{2A}(K_e + \frac{V}{\beta_m}) + s\frac{C_2M}{A} + A)}$$

Such a system can be described in terms of poles and zeros and valuable information can be obtained with an S plane plot of the position of these poles and zeros. Our case results in three poles, one at the origin and a pair of complex conjugate poles. The conjugate pole pair indicates the system is oscillatory while the pole at the origin indicates that the system may not reach the desired new setpoint or that it will have a steady state error. However, this is of little concern to us here. Plotting the zeros in Figure 31,

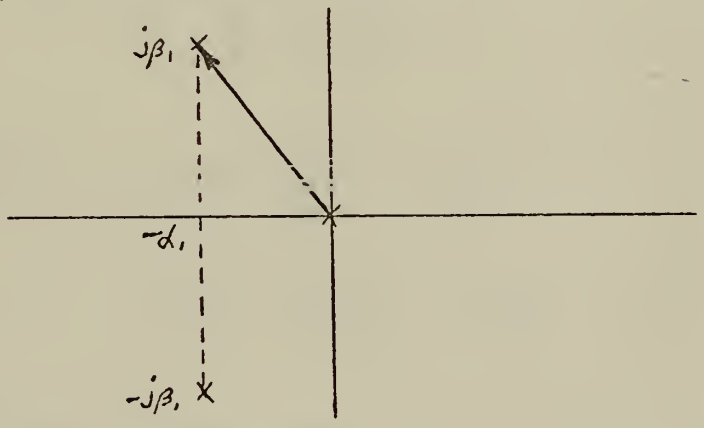

Figure 31.

The natural frequency of interest is defined by the length of the phazor connecting the origin to a complex pole. Basically, if we put the transfer function in the form

$$T(s) = \frac{\text{const}}{s(s + \alpha_1 + j\beta_1)(s + \alpha_1 - j\beta_1)} ,$$

we can adjust the natural frequency of the system by adjusting the coefficients which control the position of the complex conjugate poles.

In our case,

calling $\frac{M}{2A}(K_e + \frac{V}{\beta}) = A_2$

$\frac{M}{A}C_2 = A_1$

$A = A_0$

and rewriting

$$\overline{y}(s) = \frac{\text{const}}{s(A_2 s^2 + A_1 s + A_0)}$$

The natural frequency of the system is defined by the roots of the equation

$$s^2 + \frac{A_1}{A_2} s + \frac{A_0}{A_2} = 0,$$

or the magnitude of

$$-\frac{A_1}{A_2} \pm \sqrt{\left(\frac{A_1}{A_2}\right)^2 - 4\left(\frac{A_0}{A_2}\right)}$$

or

$$\sqrt{\frac{(\frac{A_1}{A_0})^2 + ((\frac{A_1}{A_2})^2 - 4(\frac{A_0}{A_2}))}{4}}$$

If we assume leakage is equal to zero then $C_2 = 0$ and all terms with A_1 go to zero, and the expression reduces to

$$\omega_n = \sqrt{\frac{-4A}{4(\frac{m}{2A}(K_e + \frac{V}{}))}}$$

$$\omega_n = \sqrt{\frac{2A^2}{MCK_e + \frac{V}{\beta})}} \quad .$$

To get a natural frequency of 0.03HZ or about 0.2 the argument of the square root would have to be about 0.50.

Assuming a baseline piston size of 1 ft^2 and V = 10 ft^3 using a mass of 2000 slugs and the bulk modulus of water β= 320,000 psi, the equation gives

$$0.50 \frac{1}{\text{sec}^2} = \frac{2 \text{ ft}^2}{2000 \text{ slugs } (K_e + \frac{10}{32{,}000})} ,$$

or, with proper units

$$0.50 \frac{1}{\text{sec}^2} = \frac{(144)(144)(2) \text{ in}^4}{2000 \frac{\text{lb}_f - \text{sec}^2}{\text{ft}} \quad \frac{\text{ft}}{12\text{in}} (K_e + \frac{17280 \text{ in}^3}{320{,}000\text{psi}})}$$

$$K_e \approx 497.00 \frac{\text{in}^3}{\text{psi}} .$$

Hence a compliance of about 500 $\frac{\text{in}^3}{\text{psi}}$ must be built into the system. Assuming an air accumulator with a working pressure of 278 psi and change of one psi

$$P_1V_1 = P_2V_2$$

$$278V_1 = 279 (V_1 - 500)$$

$$V_1 \approx 80 \text{ ft}^3 ,$$

which again is very large and bulky.

Fortunately, as was shown in the passive systems, this large accumulator may be made smaller by use of a higher working pressure. For example,

assume $P_1 = 2000$ psi

Area = 2 in^2

$$0.50 = \frac{2(4) \text{ in}^4}{\frac{2000 \text{ slugs } 1\text{ft}}{12 \text{ in}} (K_e + \frac{20}{320{,}000})}$$

$$K_e \approx 0.096 \frac{\text{in}^3}{\text{psi}}$$

or again, using an air accumulator at 2000 psi, one psi should change the volume

$$0.096 \frac{\text{in}^3}{\text{psi}}$$

$$P_1V_1 = P_2V_2$$

$$2000\ V_1 = 2001\ (V_1 - 0.096)$$

$$192\ in^3 = V_1$$

which is of reasonable size and is easy to build.

Actually, a working pressure somewhere between the limits discussed here would be most appropriate in order to reduce piston size and weight as well as reduce the plenum size. In short, there is probably an optimum selection of working pressure, piston area, and hydraulic fluid. A notional system employing this approach is shown below in Figure 32.

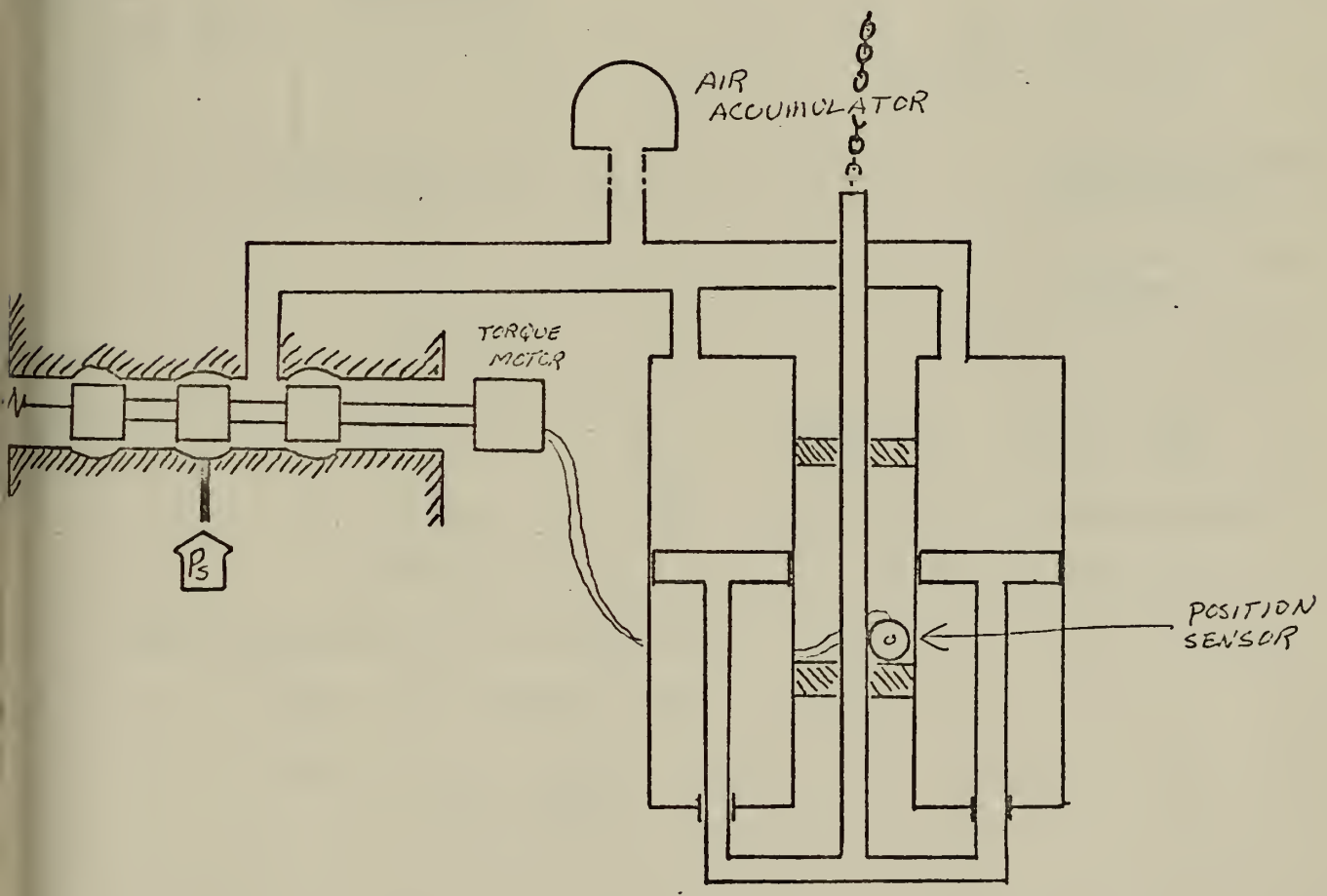

Figure 32.

A Proportional-Integral Control Approach

By increasing the level of control is include integral as well as proportional control we may be able to improve the system and possibly reduce the size of the plenum chamber.

Modeling the system as shown below the following equations result,

Figure 33.

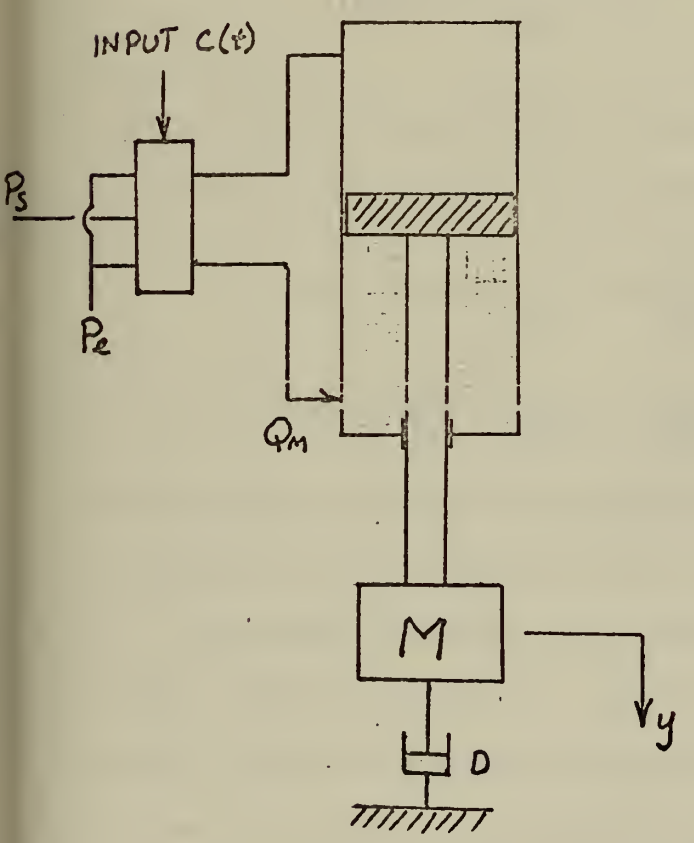

Area = A

P_m = Load pressure

K_{et} = Total fluid plus cylinder compliance

Q_m = Flow to load

$F_o \sin\omega t$ = Disturbance

R = Proportional control constant

S = Integral control constant

D = Damping constant

(1) $\dot{y} = K_{et}\dot{P}_m - \frac{Q_m}{A}$

(2) $M\ddot{y} = -P_m A - F_o \sin\omega t - D\dot{y}$

(3) $Q_m = Ry + S\int y\,dt - \dot{c}(t)$.

Combining equations (1), (2), and (3)

$$M\dddot{y} = -\dot{P}_m - F_o \omega \sin\omega t - D\ddot{y}$$

but

$$\dot{P}_m = \frac{\dot{y}}{K_{et}} + \frac{Q_m}{AK_{et}} \quad .$$

Plugging in

$$m\dddot{y} = -A\left(\frac{\dot{y}}{K_{et}} + \frac{Q_m}{AK_{et}}\right) - F_o \omega \cos\omega t - D\ddot{y}$$

also,

$$\dot{Q}_m = R\dot{y} + Sy - C(t)$$

or finally,

$$M\dddot{y} + D\ddot{y} + \frac{A}{K_{et}}\ddot{y} + \frac{R}{K_{et}}\dot{y} + \frac{Sy}{K_{et}} = \dot{C}(t) + Fow^2\sin\omega t.$$

Using LaPlace transforms,

$$\bar{y}(s) = \frac{\dot{C}(t) + Fow^2\sin\omega t}{(MS^4 + DS^3 + \frac{A}{K_{et}}S^2 + \frac{RS}{K_{et}} + \frac{S}{K_{et}}}$$

Where $\dot{C}(t)$ is the input setpoint (time rate of change) and $Fow^2\sin\omega t$ is the disturbance, the characteristic equation is then

$$MS^4 + DS^3 + \frac{A}{K_{et}}S^2 + \frac{RS}{K_{et}} + \frac{S}{K_{et}} = 0$$

or

$$S^4 + \frac{DS^3}{M} + \frac{A}{K_{et}M}S^2 + \frac{RS}{K_{et}M} + \frac{S}{K_{et}M} = 0.$$

This equation can then be analyzed with standard procedures and proper coefficients for R, S, and K_{et} can be found.

Some general comments can be made about proportional-integral versus simple proportional control. Addition of integral control allows the system to respond to a change in set point with zero steady state error while it does not change the basic natural frequency of the system. Moreover, this control element provides an additional independent constant which can be used to more accurately tune the system for maximum decoupling effect. The availability of this additional constant may well offset the complexity added with an integral feedback unit.

One fact to be aware of with the P.I. control discussed above is that the cradle has been shown to exhibit less than critical damping. Hence,

the characteristic equation would probably become unstable upon the application of a reasonable gain and additional damping may be needed. This damping could be provided either by mechanical means or by additional feedback such as velocity and acceleration.

The determination of the optimal design for such a feedback control system is left for future work.

Other Systems

Basically, all other systems are combinations of the passive and active systems. Some system modifications which may be desirable include:

(1) Inclusion of horizontal sensing valves which tend to channel fluid to the low sides of the cradle thus giving horizontal feedback to an active system.

(2) Substitution of rotary air or fluid motors with gear racks to provide the vertical position control.

(3) The utilization of an active-passive system which employs a position control to center a passive piston or rack.

CHAPTER VII.

CONCLUSIONS AND RECOMMENDATIONS

As a result of the investigations carried out in this thesis, several conclusions have been arrived at.

1. A four point passive decoupling scheme can substantially decrease ship heave, pitch, and roll transmission to a submerged cradle.

2. The effective spring constants required for decoupling fall in the range of 20-50 lb_f/ft.

3. Each mode of oscillation will couple energy into the other two modes, hence the design of a decoupling system must take each natural frequency into consideration.

4. Cradle hydrodynamic drag is a complex function of frequency, amplitude, and velocity and must be chosen to suit the individual situation which is to be modeled.

5. Conventional springs such as coil or leaf springs which will have a soft spring constant and also a large initial static load do not exist.

6. Passive pneumatic springs, while meeting desired requirements, would require large plenum chambers in order to operate at safe and reasonable pressure levels. Additionally, these passive devices would be difficult to center in the cylinder.

7. A logical approach for creation of soft springs with initial static loads would be an active feedback control system. A system, such as one utilizing proportional and integral feedback, could substantially decouple ship motions from the cradle, yet maintain the resultant piston oscillations about the center of the cylinder or set point.

In summary, both the theoretical and practical aspects of a cradle mounted decoupling system have been investigated. The value of this analysis is that it brings us to the point where we must decide whether the possible improvements in operating conditions warrant the considerable time and expense involved in making such a system come true. If the analysis had shown that a simple passive system would work and was readily available, further tests and construction would be easy to justify. On the other hand, since an active system seems to be necessary, extreme caution should be exercised prior to construction to assure that; first, proper feedback coefficients are found; and second, the necessary control components are available and are readily adaptable to the ocean environment. In addition to the above, care must be taken to insure that any resultant detailed design satisfys all safety requirements which may be imposed by WHOI, the Navy, or any other regulatory bodys.

Other means of decoupling ship-cradle motion have been, and are being evaluated. The author hopes that this work will enable WHOI to more clearly evaluate the cradle mounted system and how it compares to other methods being considered.

BIBLIOGRAPHY

1. Baumeister, T., Editor, Mark's Standard Handbook for Mechanical Engineers, 7th. Edition, McGraw Hill, Inc., New York, 1967.

2. Blackburn, Reethof, Shearer, Fluid Power Control, M.I.T. Press, M.I.T., Cambridge, MA, April 1972.

3. Cohen, Jay Martin, An Experimental Analysis of the Dynamics of a Submerged Tethered Cradle, Unpublished Manuscript, W.H.O.I.-72-45, Woods Hole, MA, June 1972.

4. Den Hartog, J.P., Mechanical Vibrations, 4th Edition, New York: McGraw-Hill Book Company, Inc., 1956.

5. Myers, Holm, McAllister, Handbook of Ocean and Undersea Engineering, McGraw-Hill, Inc., New York, 1969.

6. Newman, J. N., Marine Hydrodynamics, Unpublished Lecture Notes, Cambridge, MA: M.I.T., 1971.

7. Shultz, Melsa, State Functions and Linear Control Systems, McGraw-Hill, Inc., New York, 1967.

8. Vandiver, John K., Dynamic Analysis of a Launch and Recovery System for a Deep Submersible, Unpublished Master's Thesis, M.I.T., Cambridge, MA, 1969.

APPENDIX I.

COMPUTER PROGRAM

```
      SUBROUTINE EQSIM
      REAL I1,I2,K1,K2,K3,K4,MT,M0,M1,L
      COMMON T,DT,Y(20),F(20),STIME,FTIME,NEWDT,IFWRT,N
C
C     ALVIN, CRADLE, AND LULU DYNAMIC SIMULATION USING DYSYS
C
C     DEFINITION OF TERMS USED
C
C     Y(1) = CRADLE CENTERLINE VERTICLE POSITION  ( + IS DOWN )
C
C     Y(2) = CRADLE CENTERLINE VERTICLE VELOCITY  ( FT/SEC )
C
C     Y(3) = CRADLE PITCH ANGLE  ( RADIANS )
C
C     Y(4) = CRADLE PITCH ANGULAR VELOCITY  ( RADIANS/SEC )
C
C     Y(5) = CRADLE ROLL ANGLE  ( RADIANS )
C
C     Y(6) = CRADLE ROLL ANGULAR VELOCITY  ( RADIANS/SEC )
C
C     Y(7) = FINITE ELEMENT HEAVE DRAG TERM
C
C     Y(8) = LINEAR HEAVE DRAG TERM
C
C     Y(9) = FINITE ELEMENT PITCH DRAG TERM
C
C     Y(10) = LINEAR PITCH DRAG TERM
C
C     Y(11) = CRADLE PITCH ANGLE IN DEGREES
C
C     Y(12) = CRADLE ROLL ANGLE IN DEGREES
C
C     Y(13) = SHIP HEAVE  ( FT )
C
C     Y(14) = SHIP PITCH IN DEGREES
C
```

```
C      Y(15) = SHIP ROLL IN DEGREES
C
C      Y(16) = FINITE ELEMENT ROLL DRAG TERM
C
C      Y(17) = LINEAR ROLL DRAG TERM
C
C
C      YO = LULUS MAXIMUM HEAVE AMPLITUDE  ( FT )
C
C      THET = LULUS MAXIMUM PITCH ANGLE  ( RADIANS )
C
C      FI = LULUS MAXIMUM ROLL ANGLE  ( RADIANS )
C
C      W1 = LULUS PITCH AND HEAVE FREQUENCY  ( RADIANS/SEC )
C
C      W2 = LULUS ROLL FREQUENCY  ( RADIANS/SEC )
C
C      K1 THROUGH K4 ARE THE SPRING CONSTANTS OF THE FOUR CRADLE
C      SUPPORT SPRINGS  ( ORIGINALLY CHAIN )
C
C      PER = PERCENT DEVIATION IN SPRING CONSTANTS (%)
C
C      CD = DRAG COEFFICIENT  ( DIMENSIONLESS )
C
C      P = DENSITY OF SEA WATER  ( LBF-SEC**2/FT**4)
C
C      L = LENGTH OF CRADLE
C
C      W = WIDTH OF CRADLE
C
C      MO = MASS OF CRADLE ON LAND  ( SLUGS )
C
C      M1 = VIRTUAL MASS OF CRADLE  ( SLUGS )
C
C      MT = TOTAL EFFECTIVE CRADLE MASS
C
```

```
C      I1 = TOTAL EFFECTIVE PITCH INERTIA(INCLUDES ADDED INERTIA)
C
C      I2 = TOTAL EFFECTIVE ROLL INERTIA(INCLUDES ADDED INERTIA)
C
C      DRAG1 = THE FINITE ELEMENT DRAG(HEAVE) VALUE
C
C      DRAG2 = THE FINITE ELEMENT DRAG(PITCH) VALUE
C
C      DRAG3 = THE FINITE ELEMENT DRAG(ROLL) VALUE
C
C      DRAG1L = THE LINEARIZED HEAVE DRAG
C
C      DRAG2L = THE LINEARIZED PITCH DRAG
C
C      DRAG3L = THE LINEARIZED ROLL DRAG
C      THE VALUE OF NEWDT WILL NOW CONTROL THE PROGRAM BRANCHING
C
C
      IF(NEWDT)1,3,2
    1 READ(8,14)YO,THET,FI,W1,W2,K1,PER,MO
   14 FORMAT(8F9.3)
      DRAG1=0.0
      DRAG1L=0.0
      DRAG2=0.0
      DRAG2L=0.0
      DRAG3=0.0
      DRAG3L=0.0
      CD=1.1
      L=17.5
      W=16.3
      P=1.9903
      M1=3.14159*(W/2.0)**2*L*P
      MT=MO+M1
      I1=(MO*L*L/12.0)+(P*3.14*L**4*W)/128.0
      I2=(MO*W*W/12.0)+(P*3.14*W**4*L)/128.0
C
```

```
C      THE FOLLOWING SHOW THE FOUR SPRINGS WITH ARBITRARY DIFFPENCES
C
       K2=K1+K1*PER/100.0
       K3=K1-PER*K1/100.0
       K4=K1+PER*K1/200.0
C
C      THE FOLLOWING ARE THE COEFFICIENTS OF THE A  AND B MATRICES
C
       A21= -(K1+K2+K3+K4)/MT
       A22=-4.0*P*CD*W*L*YO*W1/(3.0*3.14*MT)
       A23=(-K1*L-K2*L+K3*L+K4*L)/(2.0*MT)
       A25=(-K1*W+K2*W+K3*W-K4*W)/(2.0*MT)
       B21=-A21
       B23=-A23
       B26=-A25
       A41=(K3*L+K4*L-K1*L-K2*L)/(2.0*I1)
       A43=(-K3*L*L-K4*L*L-K1*L*L-K2*L*L)/(4.0*I1)
       A44=-P*CD*L**4*W*THET*W1/(24.0*3.14*I1)
       A45=(-K3*L*W+K4*L*W-K1*L*W+K2*L*W)/(4.0*I1)
       B41=-A41
       B43=-A43
       B46=-A45
       A61=(-K1*W-K4*W+K2*W+K3*W)/(2.0*I2)
       A63=(-K1*W*L+K4*W*L+K2*W*L-K3*W*L)/(4.0*I2)
       A65=(-K1*W*W-K4*W*W-K2*W*W-K3*W*W)/(4.0*I2)
       A66=-P*CD*W**4*L*FI*W2/(24.0*3.14*I2)
       B61=-A61
       B63=-A63
       B66=-A65
       WRITE(5,16)K1,K2,K3,K4,CD,I1,I2,MO,MT
    16 FORMAT(6X,'K1=',F6.1,2X,'K2=',F6.1,2X,'K3=',F6.1,2X,'K4=',F6.1,2X,
      1 'CD=',F3.1,2X,'I1=',F10.0,2X,'I2=',F10.0,2X,'MO=',F7.1,2X,'MT=',
      2  F7.1///)
       WRITE(5,17)YO,W1,THET,FI,W2
    17 FORMAT(6X,'SHIP HEAVE=',F5.2,3X,'SHIP HEAVE +PITCH FREQ=',F5.2,3X,
      1'SHIP PITCH=',F5.2,3X,'SHIP ROLL=',F5.2,3X,'SHIP ROLL FREQ=',F5.2
```

```
     2//)
C
C      THIS SECTIONS WRITES THE COEFFICIENTS OF THE A MATRIX FOR BODE PLOTS
       WRITE(5,84)
       WRITE(5,13)A21,A22,A23,A25,A41,A43,A44,A45,A61,A63,A65,A66
    84 FORMAT(5X,' THESE ARE THE COEFFICIENTS OF THE A MATRIX')
    13 FORMAT(3X,12F9.5//)
       WRITE(5,89)
    89 FORMAT(3X,'ORDER IS...T,DRAG1,DRAG1L,DRAG2,DRAG2L,DRAG3,DRAG3L,
      8Y1,Y3,Y5'//)
       II=-1
C
C
C      BRANCH TO THIS POINT ONCE EACH TIME STEP
     2 CONTINUE
C
C
C      CALCULATE ROLL AND PITCH ANGLE IN DEGREES
C
C      PITCH ANGLE
       Y(11)=Y(3)*57.29577951
C      ROLL ANGLE
       Y(12)=Y(5)*57.29577951
C      LULUS HEAVE
       Y(13)=YO*SIN(W1*T)
C      LULUS PITCH ANGLE
       Y(14)  =THET*SIN(W1*T)*57.29577951
C      LULUS ROLL ANGLE
       Y(15)=FI*SIN(W2*T)*57.29577951
C
       ANGL=COS(Y(3))*COS(Y(5))
C
C      "ANGL" IS THE COSINE CORRECTION OF THE VELOCITY VECTORS
C      COMPARISON OF LINEAR AND NONLINEAR DRAGS
C
       Y1=Y(1)
```

```
      Y2=Y(2)
      Y3=Y(3)
      Y4=Y(4)
      Y5=Y(5)
      Y6=Y(6)
      CALL DRAGH(W,L,P,CD,Y1,Y2,Y3,Y4,Y5,Y6,DRAG1,ANGL)
      CALL DRAGP(W,L,P,CD,Y1,Y2,Y3,Y4,Y5,Y6,DRAG2,ANGL)
      CALL DRAGR(W,L,P,CD,Y1,Y2,Y3,Y4,Y5,Y6,DRAG3,ANGL)
C
      DRAG1L=A22*Y(2)*MT
      Y(7)=DRAG1
      Y(8)=DRAG1L
      DRAG2L=A44*Y(4)*I1
      Y(9)=DRAG2
      Y(10)=DRAG2L
      DRAG3L=A66*Y(6)*I2
      Y(16)=DRAG3
      Y(17)=DRAG3L
C
   11 CONTINUE
C
C     THE FOLLOWING IS THE MAIN CALCULATION DONE FOUR TIMES EACH TIME STEP
C
    3 F(1)=Y(2)
      F(2)=A21*Y(1)+A23*Y(3)+A25*Y(5)+DRAG1/MT+B21*YO*SIN(W1*T) +
     1  B23*THET*SIN(W1*T)+B26*FI*SIN(W2*T)
      F(3)=Y(4)
      F(4)=A41*Y(1)+A43*Y(3)+A45*Y(5)+DRAG2/I1+B41*YO*SIN(W1*T)+
     2   B43*THET*SIN(W1*T)     +B46*FI*SIN(W2*T)
      F(5)=Y(6)
      F(6)=A61*Y(1)+A63*Y(3)+A65*Y(5)+DRAG3/I2    +B61*YO*SIN(W1*T)
     3  +B63*THET*SIN(W1*T) + B66*FI*SIN(W2*T)
C
C     CALCULATION COMPLETE
      RETURN
      END
```

```
      SUBROUTINE DRAGH(W,L,P,CD,Y1,Y2,Y3,Y4,Y5,Y6,DRAG1,ANGL)
C
C     THIS SUBROUTINE CALCULATES A VALUE FOR THE HEAVE DRAG OF THE
C     CRADLE USING A 64 ELEMENT FINITE METHOD. THE VALUE IS CALCULATED
C     ONCE EACH TIME THE SUBROUTINE IS CALLED
C
      REAL L
      DIMENSION A(16),B(16)
C     THE FOLLOWING ARE THE COEFFICIENTS OF THE DRAG TERMS FOR EACH ELEMENT
C
      A(1)=L*ANGL/16.0
      A(2)=3.0*A(1)
      A(3)=5.0*A(1)
      A(4)=7.0*A(1)
      A(5)=A(1)
      A(6)=A(2)
      A(7)=A(3)
      A(8)=A(4)
      A(9)=A(1)
      A(10)=A(2)
      A(11)=A(3)
      A(12)=A(4)
      A(13)=A(1)
      A(14)=A(2)
      A(15)=A(3)
      A(16)=A(4)
      B(1)=W*ANGL/16.0
      B(2)=B(1)
      B(3)=B(1)
      B(4)=B(1)
      B(5)=3.0*B(1)
      B(6)=B(5)
      B(7)=B(5)
      B(8)=B(5)
      B(9)=5.0*B(1)
      B(10)=B(9)
```

```
      B(11)=B(9)
      B(12)=B(9)
      B(13)=7.0*B(1)
      B(14)=B(13)
      B(15)=B(13)
      B(16)=B(13)
      VELSQ=0.0
C
C     VELSQ IS THE ABS-SQUARE OF THE VELOCITY TERMS. THESE TERMS ARE ALL
C     SUMMED AND THEN MULTIPLIED BY  THE AREA,DENSITY,AND DRAG COEFFICIENT
C
      DO 1 I=1,16
      C1=A(I)*Y4
      C2=B(I)*Y6
C
C     THE VELOCITY OF QUADRANT #1
C
      VEL=Y2+C1+C2
      VELSQ=VELSQ+VEL*ABS(VEL)
C
C     THE VELOCITY OF QUADRANT #2
C
      VEL=Y2+C1-C2
      VELSQ=VELSQ+VEL*ABS(VEL)
C
C     THE VELOCITY OF QUADRANT #3
C
      VEL=Y2-C1-C2
      VELSQ=VELSQ+VEL*ABS(VEL)
C
C     THE VELOCITY OF QUADRANT #4
C
      VEL=Y2-C1+C2
    1 VELSQ=VELSQ+VEL*ABS(VEL)
      DRAG1=-P*CD*W*L*VELSQ/128.0
C
```

```
C       DRAG1 IS THE DRAG IN HEAVE AND IS RETURNED TO THE MAIN PROGRAM
C
        RETURN
        END
```

```
      SUBROUTINE DRAGP(W,L,P,CD,Y1,Y2,Y3,Y4,Y5,Y6,DRAG2,ANGL)
C
C     THIS IS THE PITCH SUBROUTINE AND IS IDENTICAL TO THE HEAVE
C     SUBROUTINE EXCEPT THAT THE ELEMENTS ARE ALL MULTIPLIED BY THEIR
C     RESPECTIVE MOMENT ARMS IN ORDER TO HAVE DRAG IN FOOT-POUNDS
C
      REAL L
      DIMENSION A(16),B(16)
      A(1)=L/16.0
      A(2)=3.0*A(1)
      A(3)=5.0*A(1)
      A(4)=7.0*A(1)
      A(5)=A(1)
      A(6)=A(2)
      A(7)=A(3)
      A(8)=A(4)
      A(9)=A(1)
      A(10)=A(2)
      A(11)=A(3)
      A(12)=A(4)
      A(13)=A(1)
      A(14)=A(2)
      A(15)=A(3)
      A(16)=A(4)
      B(1)=W/16.0
      B(2)=B(1)
      B(3)=B(1)
      B(4)=B(1)
      B(5)=3.0*B(1)
      B(6)=B(5)
      B(7)=B(5)
      B(8)=B(5)
      B(9)=5.0*B(1)
      B(10)=B(9)
      B(11)=B(9)
      B(12)=B(9)
```

```
      B(13)=7.0*B(1)
      B(14)=B(13)
      B(15)=B(13)
      B(16)=B(13)
      C=1.0
      VELAR=0.0
C
C     HERE "VELARM" IS THE  ABS-SQUARE OF THE VELOCITY MULTIPLIED BY
C
C     ITS MOMENT ARM(AT THE CENTER OF THE ELEMENT)
      DO 1 I=1,16
      AI=I
      BI=I/4
      AAI=AI/4.0
      ARM=C*L/16.0
      C1=A(I)*Y4
      C2=B(I)*Y6
      VEL=Y2*ANGL+C1+C2
      VELAR=VELAR-ARM*VEL*ABS(VEL)
      VEL=Y2*ANGL+C1-C2
      VELAR=VELAR-ARM*VEL*ABS(VEL)
      VEL=Y2*ANGL-C1-C2
      VELAR=VELAR+ARM*VEL*ABS(VEL)
      VEL=Y2*ANGL-C1+C2
      VELAR=VELAR+ARM*VEL*ABS(VEL)
      C=C+2.0
      IF(AAI .EQ. BI) C=1.0
    1 CONTINUE
      DRAG2=P*CD*W*L*VELAR/128.0
      RETURN
      END
```

```
      SUBROUTINE DRAGR(W,L,P,CD,Y1,Y2,Y3,Y4,Y5,Y6,DRAG3,ANGL)
C
C     THE ROLL DRAG SUBROUTINE.....
C
      REAL L
      DIMENSION A(16),B(16)
      A(1)=L/16.0
      A(2)=3.0*A(1)
      A(3)=5.0*A(1)
      A(4)=7.0*A(1)
      A(5)=A(1)
      A(6)=A(2)
      A(7)=A(3)
      A(8)=A(4)
      A(9)=A(1)
      A(10)=A(2)
      A(11)=A(3)
      A(12)=A(4)
      A(13)=A(1)
      A(14)=A(2)
      A(15)=A(3)
      A(16)=A(4)
      B(1)=W/16.0
      B(2)=B(1)
      B(3)=B(1)
      B(4)=B(1)
      B(5)=3.0*B(1)
      B(6)=B(5)
      B(7)=B(5)
      B(8)=B(5)
      B(9)=5.0*B(1)
      B(10)=B(9)
      B(11)=B(9)
      B(12)=B(9)
      B(13)=7.0*B(1)
      B(14)=B(13)
```

```
      B(15)=B(13)
      B(16)=B(13)
      C=1.0
      VELAR=0.0
      DO 1  I=1,16
      AI=I
      BI=I/4
      AAI=AI/4.0
      ARM=C*W/16.0
      C1=A(I)*Y4
      C2=B(I)*Y6
      VEL=Y2*ANGL+C1+C2
      VELAR=VELAR-ARM*VEL*ABS(VEL)
      VEL=Y2*ANGL+C1-C2
      VELAR=VELAR+ARM*VEL*ABS(VEL)
      VEL=Y2*ANGL-C1-C2
      VELAR=VELAR+ARM*VEL*ABS(VEL)
      VEL=Y2*ANGL-C1+C2
      VELAR=VELAR-ARM*VEL*ABS(VEL)
      IF(AAI .EQ. BI)       C=C+2.0
    1 CONTINUE
      DRAG3=P*CD*W*L*VELAR/128.0
      RETURN
      END
```

```
06          100.0       .50
   4.25     0.35        0.35        .628        .5        20.0      10.0      508.
                        1           11          31
06          100.0       .50
   4.25     0.175       0.175       1.2         1.0       20.0      10.0      508.
                        1           11          31
```

Thesis
D697 Dow

145672

The analysis and design of a ship-cradle decoupling scheme for deep submersible recovery at sea.